


2016-01-01

# Fabrication and Testing of CFRP Composites with Embedded Piezoelectric Particles for Temperature Sensing and Energy Harvesting

Emilio Tarango Valles

University of Texas at El Paso, [emiliotv@msn.com](mailto:emiliotv@msn.com)

Follow this and additional works at: [https://digitalcommons.utep.edu/open\\_etd](https://digitalcommons.utep.edu/open_etd)

 Part of the [Materials Science and Engineering Commons](#), [Mechanics of Materials Commons](#), and the [Oil, Gas, and Energy Commons](#)

---

## Recommended Citation

Tarango Valles, Emilio, "Fabrication and Testing of CFRP Composites with Embedded Piezoelectric Particles for Temperature Sensing and Energy Harvesting" (2016). *Open Access Theses & Dissertations*. 760.  
[https://digitalcommons.utep.edu/open\\_etd/760](https://digitalcommons.utep.edu/open_etd/760)

This is brought to you for free and open access by DigitalCommons@UTEP. It has been accepted for inclusion in Open Access Theses & Dissertations by an authorized administrator of DigitalCommons@UTEP. For more information, please contact [lweber@utep.edu](mailto:lweber@utep.edu).

FABRICATION AND TESTING OF CFRP COMPOSITES WITH EMBEDDED  
PIEZOELECTRIC PARTICLES FOR TEMPERATURE SENSING AND ENERGY  
HARVESTING

EMILIO TARANGO VALLES

Master's Program in Mechanical Engineering

APPROVED:

---

Yirong Lin, Ph.D., Chair

---

Norman Love, Ph.D.

---

Bill Tseng, Ph.D.

---

Charles Ambler, Ph.D.  
Dean of the Graduate School

©Copyright

by

Emilio Tarango Valles

2016

*I would like to dedicate this to my*

*Father and Mother*

*For their Support, Guidance and Love*



FABRICATION AND TESTING OF CFRP COMPOSITES WITH EMBEDDED  
PIEZOELECTRIC PARTICLES FOR TEMPERATURE SENSING AND ENERGY  
HARVESTING

by

EMILIO TARANGO VALLES

THESIS

Presented to the Faculty of the Graduate School of

The University of Texas at El Paso

in Partial Fulfillment

of the Requirements

for the Degree of

MASTER OF SCIENCE

Department of Mechanical Engineering

THE UNIVERSITY OF TEXAS AT EL PASO

December 2016

## Acknowledgements

I would like to express the immense gratitude and respect I have for my adviser, Dr. Yirong Lin from the Mechanical Engineering Department at The University of Texas at El Paso, for the encouragement and support he showed through my research and graduate coursework. I also want to thank him for sharing his knowledge and experience no matter the subject. I would also like to thank Dr. Norman Love professor from the Mechanical Engineering Department and Dr. Bill Tseng chair and professor of the Industrial Engineering Department, both from The University of Texas at El Paso. I would like to thank my college colleagues for the help inside and outside the University: Ricardo Martinez, Md Rashedul Sarker, Luis Chavez, Jorge Silva, Ricardo Garcia, Alejandra Castellanos, Carlos Garcia, Juan Duran, Jerry Reyes, Sandeep Manandhar, Cristian SantaRosa and Sergio Cordova without your presence graduate school would not have been the same. I also want to thank all of my friends for helping me during stressful moments, always supporting me and giving me some of the best laughs of my life. Team, I hope we continue this friendship until the end of times: Jonathan Adame, Eduardo Garcia, Ignacio Delgado, Oscar Moreno, Mauricio Delgado and Carlos Ruiz.

To *Laura Litvinchuk*, thank you for sharing this special journey with me. I know it is the first of many, my dear.

To *Larissa Tarango*, thank you for being the best sister and roommate I could have had. I will forever love you with all my heart.

To my *Parents*, Dios los bendiga, los quiero con todo mi corazon.

## Abstract

As a part of this world's continuous evolution and technological advancements, smart materials and functional composites have become an attractive topic. In many cases, these new functional composites are replacing the traditional engineering material due to their customizable mechanical properties. This thesis analyzes and demonstrates the signal response, sensing capabilities and structural properties from Carbon/Glass Fiber Reinforced Plastic Composites (CFRP) with embedded Lead Zirconate Titanate particles (PZT). The added PZT particles function as actuators, giving the composites a functionality. The PZT quantity inside each composite was varied to study better and characterize the mechanical and electrical properties; the variations were of 0%, 5%, 10%, 15% and 20% of the total weight percentage. The functionality is then demonstrated by setting up custom pyroelectric and piezoelectric tests; the sensing capability is observed at the cost of some mechanical properties. The mechanical properties including strength, stiffness, toughness and density were obtained by applying the appropriate ASTM standards. The composites are fabricated using a modified autoclave molding procedure that adapts the vacuum bag method. The CFRP composite is composed of three woven glass fiber laminas sandwiched by three woven carbon fiber laminas on each side. The PZT wt.% is embedded onto the System 2000 resin that is used as the matrix. The thesis demonstrates that the CFRP composite with PZT powder gains a function at the cost of some mechanical properties. This obtained function categorizes the CFRP composites a functional material, also as the wt.% is increased a better sensing response is obtained but still at the cost of mechanical property decay. The functional composites created can be utilized in the fields of energy harvesting, temperature sensing, and structural health monitoring.

## Table of Contents

	Page
Acknowledgements . . . . .	v
Abstract . . . . .	vi
Table of Contents . . . . .	vii
List of Tables . . . . .	ix
List of Figures . . . . .	x
<b>Chapter</b>	
1 Introduction . . . . .	1
1.1 Materials . . . . .	5
1.1.1 Matrix Constituent . . . . .	5
1.1.2 Ceramic Matrix Composite (CMC) . . . . .	6
1.1.3 Metal Matrix Composite (MMC) . . . . .	6
1.1.4 Polymer Matrix Composite (PCM) . . . . .	6
1.1.5 Reinforcing Constituent . . . . .	6
1.1.6 Fiber Reinforcements . . . . .	7
1.1.7 Particulate Reinforcement . . . . .	7
1.2 Sensing Effects . . . . .	9
1.2.1 Piezoelectric Effect . . . . .	10
1.2.2 Pyroelectric Effect . . . . .	11
1.2.3 Curie Temperature . . . . .	12
1.2.4 Dielectric Material . . . . .	12
1.3 Manufacturing Process . . . . .	12
1.3.1 Prepreg . . . . .	13
1.3.2 Hand Layup . . . . .	13
1.3.3 Autoclave . . . . .	13
1.4 Carbon Fiber/Glass Fiber Reinforced Plastic Composites . . . . .	14
1.5 Quality and Imperfections . . . . .	14

1.6	Thesis Scope . . . . .	16
2	Fabrication . . . . .	17
3	Methodology and Instrumentation . . . . .	23
3.1	Dispersion . . . . .	24
3.2	Three Point Bending Tests . . . . .	24
3.3	Constituent Volume fractions and Density Calculations . . . . .	26
3.3.1	Density . . . . .	26
3.3.2	Volume Fraction . . . . .	26
3.4	SEM and Digital Microscope . . . . .	28
3.5	LCR Meter . . . . .	29
3.5.1	Natural Frequency . . . . .	29
3.6	Signal Response Set Ups . . . . .	31
3.6.1	Piezoelectric and Pyroelectric . . . . .	31
3.6.2	Piezoelectric Effect . . . . .	31
3.6.3	Pyroelectric . . . . .	32
4	Results . . . . .	36
4.1	Mechanical Characterization Results . . . . .	36
4.1.1	Density . . . . .	36
4.1.2	Volume Fraction . . . . .	37
4.1.3	Dispersion Analysis . . . . .	37
4.1.4	Three Point Bending Results . . . . .	39
4.2	Electrical Characterization Results . . . . .	40
4.2.1	Piezoelectric Effect for Energy Harvesting . . . . .	41
4.2.2	Piezoelectric for Structural Health Monitoring . . . . .	42
4.2.3	Pyroelectric for Energy Harvesting - Charge Generated . . . . .	43
4.2.4	Pyroelectric for Temperature Sensing . . . . .	43
5	Conclusion and Future Work . . . . .	48
	References . . . . .	49
	Curriculum Vitae . . . . .	53

## List of Tables

1.1	Advantages and Drawbacks of PCM . . . . .	7
1.2	Thermoset vs Thermoplastic Polymers . . . . .	7

## List of Figures

1.1	Matrix and reinforcement composites configurations. . . . .	1
1.2	Carbon Laminate in the Boeing 787 Dreamliner. . . . .	2
1.3	Functional Material Schematic . . . . .	3
1.4	Applies areas for Multifunctional Structural Composites . . . . .	4
1.5	Fiber Orientation Schematic (Left) Unidirectional (Centered) Bidirectional (Right) Random Whiskers . . . . .	8
1.6	Particulate Reinforcement(Left) Combination (Right) . . . . .	8
1.7	Piezoelectric and Pyroelectric Variables . . . . .	9
1.8	Piezoelectric and Pyroelectric Constitutive Equations . . . . .	10
1.9	Piezoelectric Effect Schematic . . . . .	10
1.10	Pyroelectric Heating Schematic . . . . .	11
1.11	Pyroelectric Cooling Schematic . . . . .	11
1.12	Hand Layup Schematic . . . . .	13
1.13	Autoclave Schematic . . . . .	14
1.14	(a) Woven Carbon Fiber Lamina (b) CF/GF Composite Set Up . . . . .	15
1.15	Carbon Fiber Reinforced Plastic (CFRP) Defect. . . . .	15
1.16	Flexure Tested CFRP Delamination [34]. . . . .	15
2.1	Vacuum Bag Setup . . . . .	17
2.2	Variations on PZT wt.% . . . . .	18
2.3	Glove Box . . . . .	19
2.4	Fiberglass System 2000Resin and 2020 Hardener . . . . .	20
2.5	Epoxy Schematic . . . . .	20
2.6	Vacuum Bag Layers and Material . . . . .	21
2.7	CFRP Sectioned plate . . . . .	22
2.8	CFRP Cut Cross section . . . . .	22
2.9	Modified Tile Cutter . . . . .	22

3.1	Three Point Bending Schematic . . . . .	24
3.2	Instron 8801 Machine . . . . .	25
3.3	Hitachi TM-1000 Tabletop Microscope . . . . .	28
3.4	Digital Microscope . . . . .	28
3.5	LCR Meter . . . . .	29
3.6	CFRP Composite Cantilever Beam Set Up for SHM . . . . .	30
3.7	Hand held Heat Gun for Pyroelectric test . . . . .	32
3.8	Hand held Heat Gun for Pyroelectric test . . . . .	33
3.9	Hotplate for Pyroelectric setup . . . . .	33
3.10	Silicone Rubber Heating pad for Pyroelectric setup . . . . .	33
3.11	Controlled Tube Furnace for Pyroelectric setup . . . . .	34
4.1	CFRP Composite Density . . . . .	36
4.2	CFRP Composite Fiber Volume Fraction . . . . .	37
4.3	CFRP Composite Surface Dispersion . . . . .	38
4.4	CFRP Composite Cross Sectional View . . . . .	38
4.5	Stress-Strain Curve and Bending Modulus . . . . .	39
4.6	CFRP Composite Maximum Strength (Left) and Strain at that point (Right)	40
4.7	CFRP Composite Toughness (Area under the Load-Displacement Curve) . .	41
4.8	CFRP Composite Piezoelectric Constant . . . . .	42
4.9	CFRP Composite SHM for 0 wt.% . . . . .	43
4.10	CFRP Composite SHM for 20 wt.% . . . . .	43
4.11	CFRP Composite Charge under Temperature Cycles . . . . .	44
4.12	CFRP Composite PZT Plate Response . . . . .	44
4.13	CFRP Composite 10 wt.% Response . . . . .	45
4.14	CFRP Composite 10 wt.% Temperature Calculation . . . . .	45
4.15	CFRP Composite 10 wt.% Temperature Calculation . . . . .	45
4.16	CFRP Composite Poled Sample 1 Tubefurnace Test Data . . . . .	46
4.17	CFRP Composite Poled Sample 2 Tubefurnace Test Data . . . . .	46
4.18	CFRP Composite Non-Poled Sample 1 Tubefurnace Test Data . . . . .	47



4.19 CFRP Composite Non-Poled Sample 2 Tubefurnace Test Data . . . . . 47

# Chapter 1

## Introduction

The world is constantly evolving with technology and science, as a part of this continuous evolution material composites have become a popular topic. The definition for composites is the combination of two or more materials, that possess different mechanical properties between each other. Due to the combination of these materials a new material emerges that exhibits the best qualities of their constituting component plus qualities that neither constituting material possess [24]. There are two main categories in composites these classified as the reinforce and the matrix shown on Figure 1.1. In the last two decades, the use of composite materials on engineering applications ranging from air, space and water aircrafts and structures to automotive and biomedical has greatly increased [3]. The field of composites continues to achieve scrutiny and claims the attention and imagination of scientist and engineers. This material has in many cases replaced traditional engineering materials like steel and aluminum and one of the main reasons they are being preferred over the traditional materials is because they offer excellent strength/stiffness-to-weight ratios, they are corrosion and chemical attack resistant, exhibit good electrical behaviors and usually are low maintenance and sustainable. [5].

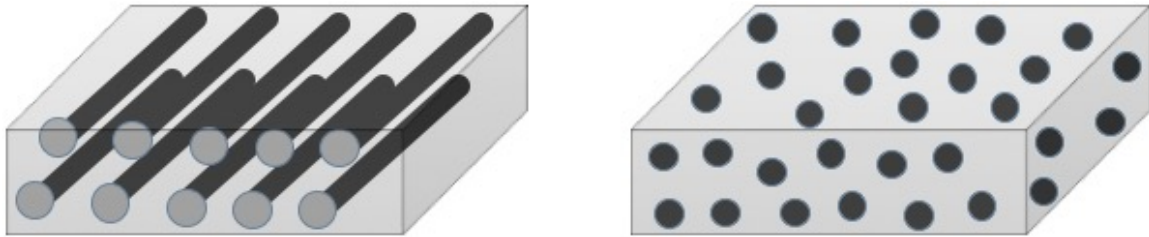


Figure 1.1: Matrix and reinforcement composites configurations.

The idea and concept of composites have been around for many years a clear reason being that Mother Nature utilizes them, the oldest composites are those that are natural,

some examples are wood and bone [2]. The bone inside our body is a hierarchical nanocomposite that is built from ceramic tables and organic binders it is of course completely natural. [5]. The bone is made from a hard but brittle material called hydroxyapatite which is composed primarily of Calcium Phosphate and Collagen which is a flexible and soft material that is a protein. The combination of the two generates the perfect material for the human skeleton. The first and most rudimentary use of human-made composites go back to reinforced clay and pottery utilizing mud as the binder. In ancient Egypt, the combination of materials such as clay and thick mud with chopped straw or cane as reinforcements was used for construction [7] [10]. A more modern use of composite materials consists of metal, ceramic or polymer binders reinforced with different particles or fibers [4]. As an example of these advantages, the Boeing 787 Dreamliner utilizes carbon fiber reinforcements on the air-frame and primary structure, this offers weight savings on the average of 20% compared to conventional aluminum designs. The Dreamliner is 50% composite by weight [4].



Figure 1.2: Carbon Laminate in the Boeing 787 Dreamliner.

As composites are becoming more and more a part of our modern life and will continue to be a role player in future projects, technology, and research must be implemented on them. A method of doing this is adding an enabling material that will yield a reasonable decay in the first mechanical properties to achieve and obtain an extra function; this has generated a new term called functional composites. It has given functional composite the

ability to have the desirable traditional composite mechanical advantages plus a beneficial effect. This enabler has made them an important and crucial role for present and future technologically advanced projects, as well unlocking new design concepts that were not possible before. Functional Composites are being commonly used in transducer applications; they are also being used to improve acoustic, thermal, mechanical, optical and electrical signal performance of piezoelectric devices and many more applications.[35]. The common enabling materials as seen in Figure 3. are Piezoelectric, Pyroelectric, and Ferroelectric materials to apply these composites to the fields of energy harvesting, structural health monitoring and sensing fields via the Piezoelectric and Pyroelectric effects. Through these, the composites are being utilized as embedded transducers, temperature sensors, and SHM sensors by converting physical and thermal variations into an electrical output that can be analyzed, self-healing some other applications seen on 1.4

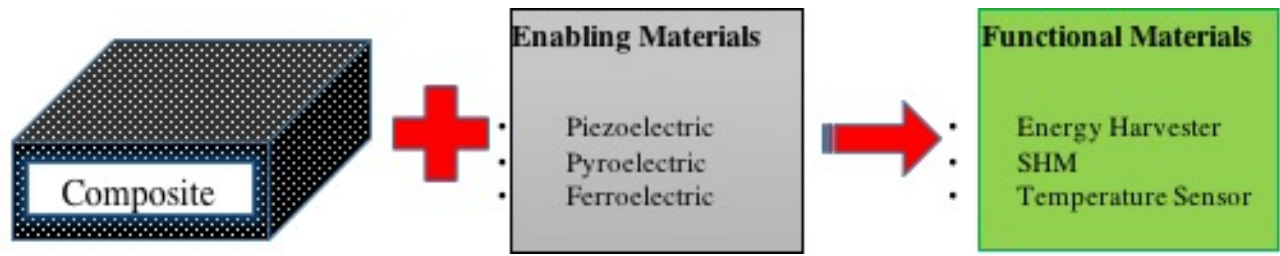


Figure 1.3: Functional Material Schematic

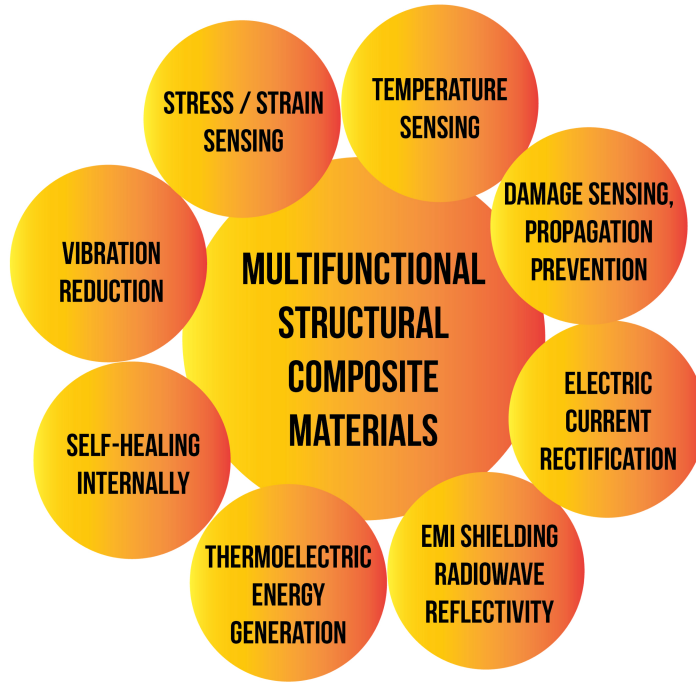


Figure 1.4: Applies areas for Multifunctional Structural Composites

Additionally, the environmental impact and aspect of energy harvesting to power low-energy consumption systems is becoming a growing topic due to the efficiency increase they can provide. In research, some of the existing systematical methods for energy harvesting are: Piezoelectric expressed as vibrations sensor or SHM sensors, Pyroelectric meaning thermal energy variation for temperature sensors, Thermoelectric defined as thermal energy gradient and Photovoltaic which usually are semiconductor devices such as solar cells [30]. Pyroelectricity has developed and grown in the area of sensors and its applications; it has revealed it can be used as a robust and useful source of energy. Although pyroelectric efficiencies are not ideal and considered low, studies have shown that pyroelectric cells can produce currents in the order of  $10\text{E-}7$  Amps, and charges on the order of  $10\text{E-}5$  C for temperature fluctuations from 300 K to 360K [30]. However, for most of the functional materials researched the use of ceramic plates like Lead Zirconate Titanate also known as PZT, has always been used. For this thesis, the merging of PZT powder on to the CFRP matrix will be studied because the amount of articles that have been published for functional composites via PZT powder

is minimal. Woven carbon fiber reinforced plastic (CFRP) composites were selected to be tested with the addition ceramic spheres of PZT. These were manufactured at The University of Texas at El Paso Challenger-Columbia laboratory and where then their mechanical and electrical properties were tested. This thesis utilizes the Piezoelectric effect for the structural health monitoring (SHM) and energy harvesting profile while the Pyroelectric effect is used for temperature sensing. The sensing capabilities experimented and energy harvesting possibility will benefit the construction, aeronautic and automobile industries by having smarter maintenance cycles, reduced downtime, energy efficiency, having a green energy approach, and preventing failure during operation [19]. Even through all the benefits and great merits that composites offer they consist of multiple layers called laminas these are subjected to failure due to several factors for example delamination, moisture absorption, and low-speed impact[2]. Because of that the need for more sophisticated structural health monitoring and nondestructive evaluations (NDE) or nondestructive inspections (NDI). These mentioned sensors can effectively determine the failure or abnormalities of a structure but can also be utilized to monitor its health for part rotation or replacement continuously. As mentioned before the advantage these sensors offer is that they provide an extra safety feature to the design by detecting any abnormality. This faster detection time can provide a larger period to work out a solution and take action.

## **1.1 Materials**

### **1.1.1 Matrix Constituent**

The matrix material is the continuous phase in the composite, and it carries several functions. It acts as an adhesive to keep the reinforcing materials in place. Thus it functions as a controller to uniformly distribute the applied load to the reinforcing material [36]. It carries some of the load more so transverse stress, intralaminar shear stress and bearing stress, because of these features some mechanical properties are dominated by the matrix [4]. The matrix deeply determines the heat and electrical conductivity, the temperature ranges in which the composite will operate. The matrix material can also protect the reinforcing materials from mechanical damage or chemical attack and gives it the overall external characteristics. The interaction between both phases, meaning how well they attach, is

also a critical aspect that affects the mechanical properties and overall quality [22]. Matrix materials can be polymers, metals or ceramics.

### **1.1.2 Ceramic Matrix Composite (CMC)**

These type of composites are commonly used in atomic energy and aerospace industries, they are utilized in extremely high-temperature environments, they use a ceramic as the matrix and then reinforce it via whiskers or short fibers of different materials. The materials are combined via covalent and ionic bonds or a mixture of the two. An example of this is SiC-Fiber-reinforced/SiC matrix composite that has non-substitutable applications as a thermal component, due to its preferred radiation and thermal properties [9].

### **1.1.3 Metal Matrix Composite (MMC)**

These composites are used for several applications, but they have become attractive candidates to the automotive industry. It is a result of the combination of the metal element bonds that make them have low cost and isotropic behavior. They present creep and fatigue resistance and high tensile strength. [16].

### **1.1.4 Polymer Matrix Composite (PCM)**

These composites mix a polymer resin with a catalyst to being the solidification process called the curing process. Several types of resins and epoxy's are utilized, each polymer has different qualities; therefore the selection is handled as a case by case scenario, and it truly depends on the composite environment. The difference in resin selection are shown on 1.1.4. [13] [12] [26].PCM are also divided by thermoplastic and thermoset polymers, the difference between the both can be an observer in Table 2.

### **1.1.5 Reinforcing Constituent**

The other constituent is the reinforcing phase which is the one embedded in the matrix and usually is the one that carries the most amount of load; the composite will now acquire stronger mechanical properties along the reinforcing direction. There are several forms the reinforcing material can be present: fibers and particles. Although the reinforcing material is

Table 1.1: Advantages and Drawbacks of PCM

Name	Advantage	Drawback
Polyesters	Low Costs Ability to be made translucent	Ceiling Temperature of 170 °F Brittleness High Shrinking during curing
Phenolics	Low Cost Mechanical Strength	High Void Content
Epoxies	High Mechanical Strength Adherence to Metals and Glass	High Cost Difficult processing

Table 1.2: Thermoset vs Thermoplastic Polymers

Thermoset	Thermoplastic
High Strain in failure Indefinite Shelf Life Short Cure Cycles Excellent Solvent Resistance	Low Strain in failure Cannot be Reprocessed Long Cure Cycles Fair Solvent Resistance

to increase mechanical properties some degrade through the perpendicular direction of fibers commonly known as the transverse direction, ductility, and fracture toughness [19] [15].

### 1.1.6 Fiber Reinforcements

Fibers can be considered the principal reinforcing component in the reinforcing constituent phase. They are the highest volume fraction component in the composite and share the most portion of the load acting on the structure [23]. Different types of fiber reinforcements exist some examples consist of short fibers, platelets, whiskers or long fibers long fibers can be unidirectional, bidirectional or randomly oriented as shown in Figure 4. The transverse strength of high toughness composites is generally low [28] [33].

### 1.1.7 Particulate Reinforcement

Particulate reinforcements are minuscule particles that are embedded in the composite matrix phase; they vary in shapes and sizes. The common reinforcers are nearly spherical, cubic or tetrahedral. Particulates are often used at fillers, as a result of this the volume fraction of the matrix is lowered and thereby produces a reduction in cost, particularly in



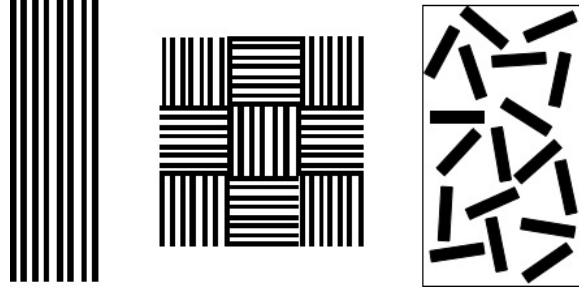


Figure 1.5: Fiber Orientation Schematic (Left) Unidirectional (Centered) Bidirectional (Right) Random Whiskers

scenarios where the matrix is costlier than the particulate [? ]. Particulate reinforcers can be considered heterogeneous in nature, but they maintain a predominant isotropic mechanical and physical behavior [33]. The interaction between the particulate and matrix materials must be taken into account as not every material would benefit the structure, which positive or negative interaction limits the material selection for particulate reinforcers. As an example if the particle corrodes or reacts to the matrix or if it absorbs too much of the matrix it would not be cost effective [28] The size of the particle and distribution matters as they produce stress concentration through the composite. They are not utilized where strength is a critical attribute since the purpose is to increase matrix properties, thermal and electric conductivity, growth in wear and abrasion resistance but most importantly reduce cost [? ] These can also be combined with fiber reinforcers and are represented in Figure 5.

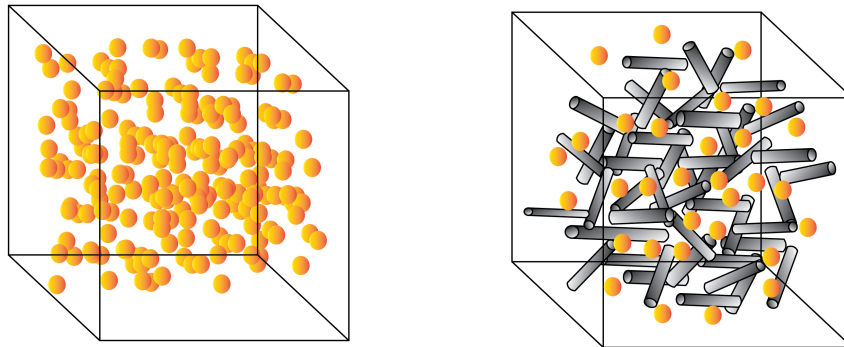


Figure 1.6: Particulate Reinforcement(Left) Combination (Right)

## 1.2 Sensing Effects

As time passes engineers continue to develop and improve technology and apply it into composites. This combination of composites and technology, as stated before creates Functional Composites. The way they have managed is by incorporation piezoelectric, pyroelectric and ferroelectric materials into the composites via ceramic plates or fiber reinforcers. The addition of these materials lowers the mechanical properties of the structure but enables them to have a sensing capability i.e. a sacrifice in mechanical properties provides the composite to attain electrical sensing. This sensing capability allows functional composites to be applied as sensors, transducers and energy harvesters. The physical behavior of piezoelectric ceramics involves heat, mechanical and electrical effects. The best representation of these variables are simplified in the Heckman diagram 1.7. In this figure, electrical field ( $E$ ), temperature ( $t$ ), and stress ( $T$ ) are interrelated with charge flux ( $D$ ), entropy ( $s$ ), and strain ( $S$ ). From the interaction among these variables the piezoelectric, pyroelectric, and thermomechanical effect are represented. The constituent equations in matrix form are represented in 1.8.

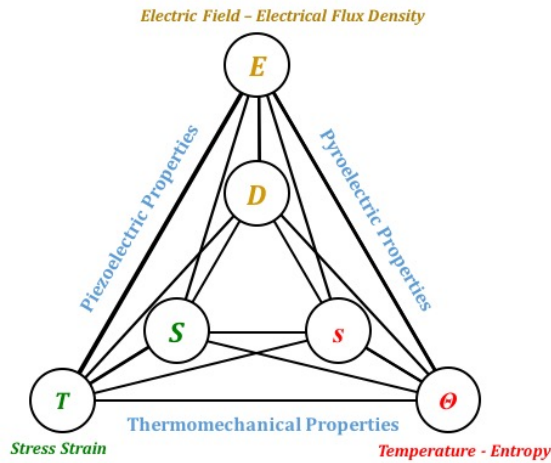


Figure 1.7: Piezoelectric and Pyroelectric Variables

$$\begin{bmatrix} \Delta\sigma \\ D_i \\ S_\lambda \end{bmatrix} = \begin{bmatrix} \frac{\rho c^{E,T}}{\Theta} & p_j^T & \alpha_\mu^E \\ p_i^T & \varepsilon_{ij}^{\theta,T} & d_{i\mu}^\theta \\ \alpha_\lambda^E & d_{j\mu}^\theta & s_{\lambda\mu}^{\theta,E} \end{bmatrix} \begin{bmatrix} \Delta\theta \\ E_j \\ T_\mu \end{bmatrix}$$

$p_i^T$ : Pyroelectric     $\varepsilon_{ij}^{\theta,T}$ : Dielectric     $d_{i\mu}^\theta$ : Piezoelectric  
 $s_{\lambda\mu}^{\theta,E}$ : Compliance     $\alpha_\lambda^E$ : Thermal Expansion

Figure 1.8: Piezoelectric and Pyroelectric Constitutive Equations

### 1.2.1 Piezoelectric Effect

The word piezoelectric is derived from the Greek word Piezo which means pressure and Electron meaning amber anciently known as a source of electric charge. The piezoelectric effect is the ability of certain crystalline materials to generate an electrical charge output proportional to a mechanical stress input [17]. In many materials the crystal unit cell is symmetric for example metals, however for piezoelectric materials it is not. Piezoelectric material crystal unit cell is not symmetric, but the electrical charges are perfectly balanced, by pressuring the material crystals they become strained and the atoms are moved. Atom movement called dipole movement creates an unbalancing of the electrical charge, therefore, causing an electrical charge to appear [6] [20]. This effect makes piezoelectric materials ideal for sensors, transducers and energy harvesters [29]. There are human-made piezoelectric ceramics utilized in the field some are PZT (Lead Zirconate Titanate), Barium Titanate and Lithium Niobate. In a more basic explanation piezoelectric materials transfer mechanical energy into electrical energy, a piezoelectric effect schematic is represented in Figure 7 [21].

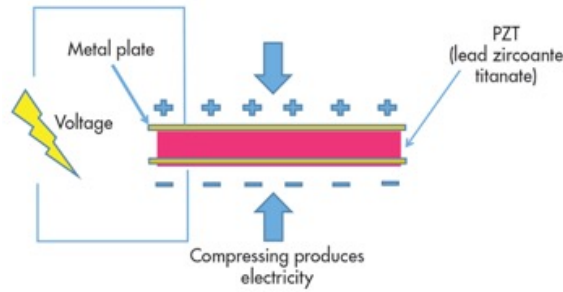


Figure 1.9: Piezoelectric Effect Schematic

### 1.2.2 Pyroelectric Effect

Similar to piezoelectric pyroelectric is a Greek derived word the change is Pyro meaning fire. Pyroelectric materials have the ability to produce a temporary voltage when they are subjected to a change in temperature with respect to time. The change in temperature creates a dipole movement through the crystal of the material [32]. The dipole movement is due to a polarization change generated inside the material thus generates the unbalance in charge and creating the electrical charge, this polarization is called the Maxwell-Wagner polarization [38]. In a more simplistic manner pyroelectric material transfers thermal energy into electrical energy. The applications for pyroelectric materials are similar to those for piezoelectric, sensors and energy harvesters. Temperature change can either be heating or cooling as it can be in cycles [29], this can be seen in Figure 8.

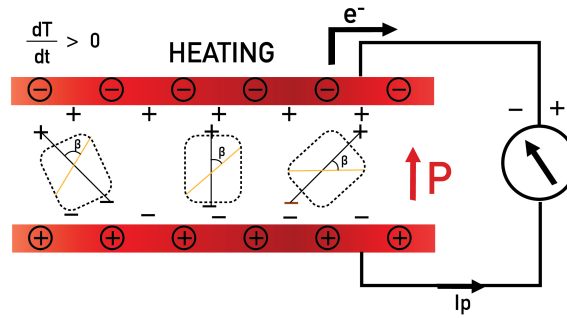


Figure 1.10: Pyroelectric Heating Schematic

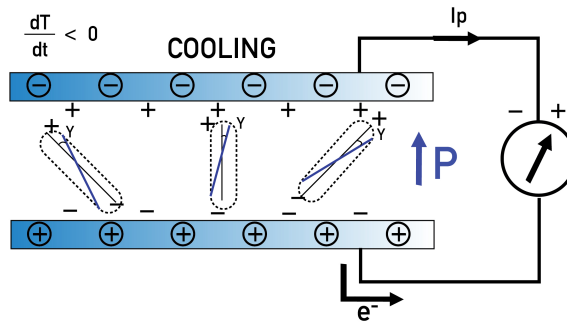


Figure 1.11: Pyroelectric Cooling Schematic

### 1.2.3 Curie Temperature

In the piezoelectric and pyroelectric material world, there is critical boundary condition that must be taken into account. This boundary condition is called the Curie temperature when a piezo/pyro material exceeds this is the temperature point in which the elements start to lose their properties [17]. Above the transition temperature, the material unit cells are symmetrical therefore the dipole movement, instant polarization and cancels the net charge polarization. Piezoelectric materials and pyroelectric materials all have instant electric polarization below career point [11]. Therefore we must not exceed this temperature in the CFRP composite; this is not possible due to the epoxy material used no being able to go above the Curie temperature of PZT that is 400 C. Changes in the material composition changes the Curie temperature setting. Therefore it is an individual property of each material[14], if the temperature is exceed the material starts to behave as a dielectric material having no electric polarization.

### 1.2.4 Dielectric Material

The CFRP composites have a dielectric material in the middle of them, as mentioned before this is a capacitor style setup that consists of glass fiber acting as a dielectric material in between the carbon fiber layers. Dielectric materials are commonly used in charge storage devices [31] and the combiantion of these amterials with piezoelectric and pyroelectric materials is also commonly used [37]. Dielectric materials increase the capacitance and therefore electric charge storage is also growing. Due to that reason, the glass fiber was used to mimic the commercial capacitors and enhance the capacitance of the composite[25].

A capacitor works by having a charge stored in between two plates (carbon fiber lamina's) the amount of charge depends on the voltage, current and capacitance.

## 1.3 Manufacturing Process

There are several manufacturing methods in existence for composites each on has positive and negative attributes [18] The common ones will be individual discussed.

### 1.3.1 Prepreg

This style of the matrix is a ready to go type of fiber mat, it consists of an adhesive embedded between the fibers. This makes the manufacturing process less time consuming, and it becomes hassle free. These can now be stacked or layered to manufacture the composite, and are stored in different environments depending on the polymer and polymer type [19]. Most high performing composite components are being produced via Epoxy Prepreg in autoclave manufacturing method [1].

### 1.3.2 Hand Layup

This process is the simplest of them all it consists of manually laying the reinforcing fibers into the desired mold. The advantages this process presents are the extremely low tooling costs the high design flexibility with regards to shape and size. The downside to this method is that each mold can only be used for a specific layout. Figure 9 graphically represents this process. The operator must take into account safety precautions in the applications of resin [22] since this is done manually. A brush may be used to apply the resin as well as a spray gun; extra precaution must be given to the first layer with regards to alignments and air bubbles.

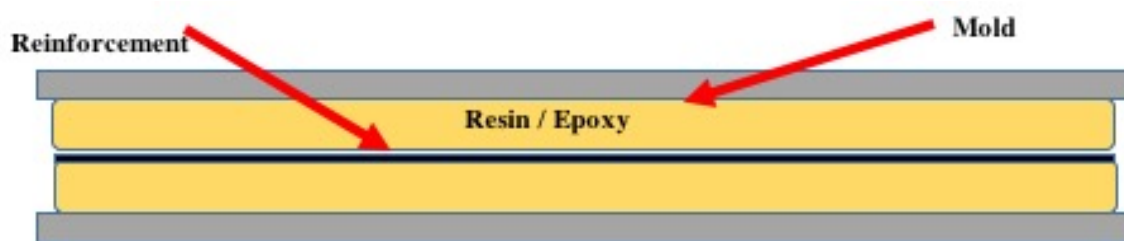


Figure 1.12: Hand Layup Schematic

### 1.3.3 Autoclave

This manufacturing method is especially utilized for high pressure and high temperature, some decades ago this was the main manufacturing method, but many outside of autoclave methods have arisen for example vacuum bag. The cost of this set up is costlier than the hand lay-up due to the generation of a mold, a system to heat it and a system to

apply the pressure. The system utilizes convection heating and comparing it to the rest of the processes this is the faster than the rest making it in some cases worth the extra cost [1] Figure 9 depicts an autoclave system image.

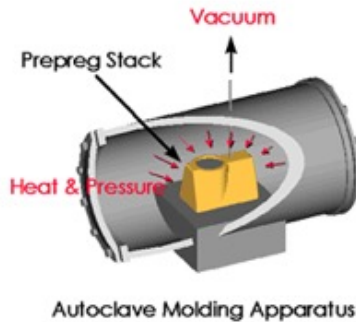


Figure 1.13: Autoclave Schematic

#### 1.4 Carbon Fiber/Glass Fiber Reinforced Plastic Composites

Carbon fiber and Glass fiber are used separately and individually for many aerospace, aviation, and land vehicles as well as construction structures. They are composed of many grouped individual layers called Laminas these represent a fundamental building block figure 10 (a) [27]. A Laminate is a group or collection of laminas that are stacked to achieve the desired mechanical properties via stiffness and thickness [8]. The spacing between the laminas is called the Interlaminar region and is a matrix (resin) rich region, therefore due to the low mechanical properties the matrix has, the Interlaminar region is usually the point of failure. The set-up this thesis utilizes is carbon fiber and glass fiber combined; the purpose is to use the highly conductive carbon fiber as an electrode and the glass fiber sandwiched in between as the dielectric material to form a capacitor type set up Figure 10 (b)

#### 1.5 Quality and Imperfections

Composite have a different type of failure conditions that ranges from delamination to void content during fabrication. Each composite is designed for a specific task, and they each have a different pre-determined failure condition. As an example is having many fiber

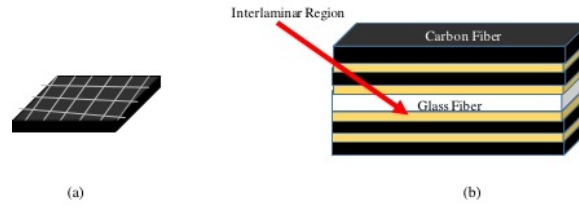


Figure 1.14: (a) Woven Carbon Fiber Lamina (b) CF/GF Composite Set Up

in the same direction i.e. unidirectional or having laminas stacked in different orientations for a desired orthotropic response. The following figures are images of these types of failure [34].

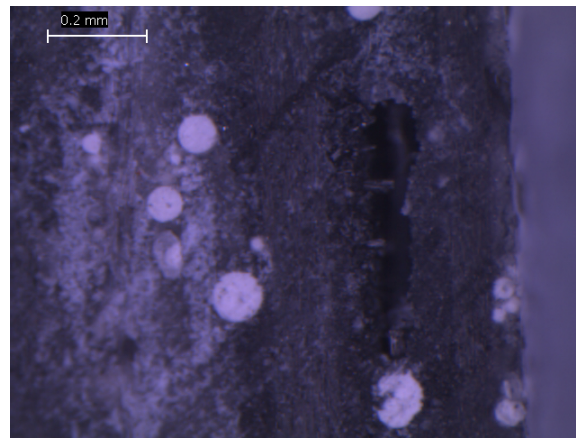


Figure 1.15: Carbon Fiber Reinforced Plastic (CFRP) Defect.

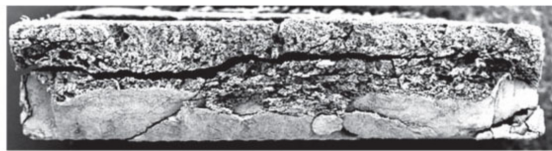


Figure 1.16: Flexure Tested CFRP Delamination [34].



## 1.6 Thesis Scope

Strong literature review on composites has shown the embedding of ceramic plates of piezoelectric/pyroelectric material to develop transducers and energy harvesters. However, these generate design limitations and provide a significant decay in mechanical properties. Those reasons have motivated this thesis to replace the ceramic plate with ceramic spheres for the same applications, in essence, fulfilling the same results with a lower mechanical property decay on the structure. Also disabling some of the previous design limitations i.e. adding curvature to the sensors. Implementation of experiments and research to the many applications multifunctional composites with the addition of piezoelectric and pyroelectric material have. The interaction between woven, carbon and glass, fibers in the same composite to generate a capacitor type set up were three laminas of glass fiber are sandwiched via three carbon fiber laminas respectively on each side. The thesis will take this capacitor type composite and embed distributed PZT (Lead Zirconate Titanate) spheres into the matrix phase, therefore, making it a multifunctional material composite; variations in the weight percentage will be generated to determine an efficient level and exhibit a distinction in enhancement. This enhanced composite will be the subjected characterization testing, pyroelectric testing, piezoelectric testing as well as impedance testing. The purpose of various tests is to determine future applications and prove their feasibility. The pyroelectric tests will be done with different heating elements to characterize; charge generated for energy harvesting and the temperature sensing capability. One piezoelectric test consists of applying a load via an Instron fatigue machine to see the charge generated. The SHM (Structural Health Monitoring) test developed utilizes electrical impedance measured by an LCR meter, the variation of impedance will demonstrate a change in the structure, therefore, creating a monitored structure.

## Chapter 2

### Fabrication

The fabrication process utilized in this thesis is a modified approach that combines the pressure aspect of autoclave molding and the manual hand lay-up procedure for vacuum bag molding 2.1

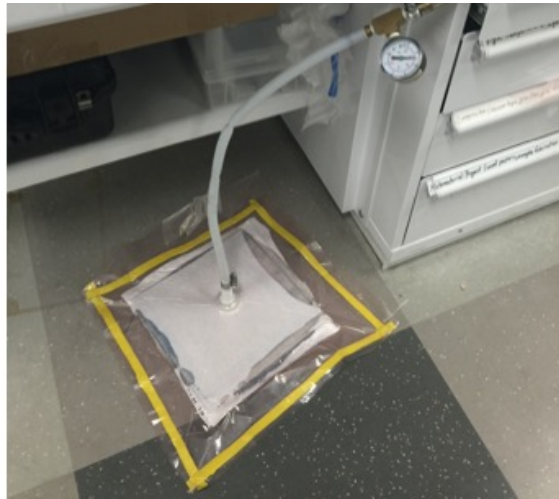


Figure 2.1: Vacuum Bag Setup

The preparation of 10 x 10 squares for the size of the woven glass and carbon fibers are traced with a silver marker. During that marking process, the woven fibers are stretched out, so the intersections between threads are completely 90 degrees, by utilizing adequate measuring tools, the woven fibers end up with precise measurements. After the fibers are correctly marked they are hand cut by utilizing specialized scissors designed for carbon fiber fabrics. The cut samples are then visually inspected to verify that they are clear and free of any other material or objects. This action is done to prevent any discrepancies during testing and data analysis, bearing us the most accurate results. Each laminate is created with nine laminas (layers) with six of the laminas being woven carbon fiber and three woven glass fiber. The total weight of these nine woven fibers is obtainable by the usage of a digital scale.

The measured total weight is then utilized to find the corresponding quantity of PZT (Lead Zirconate Titanate). The selected material was APC 840 PZT powder which particle size varied between 15 to 35 microns. In this study, the weight percentage of PZT was ranged from zero to twenty in five percent increments meaning 0%, 5%, 10%, 15% and 20% seen on 2.2. The total weight of the woven fibers is then multiplied by the percentage desired; this equals to the amount of APC 840 PZT particles embedded into the composite matrix. The APC 840 PZT powder must not be handled as any regular powder as it is toxic and harmful. Due to the fine grain size ranging from 15 to 35 microns because of this, the powder can easily drift when exposed to air and precautions were taken. During this study, the PZT weight measurement was attained inside a glove box 2.3. The reasons for the glove box utilization were those of safety, the wind protection it provides ensure the entire amount goes to the desired place as well as the prevention of inadvertent inhaling. The powder is then mixed with the epoxy.

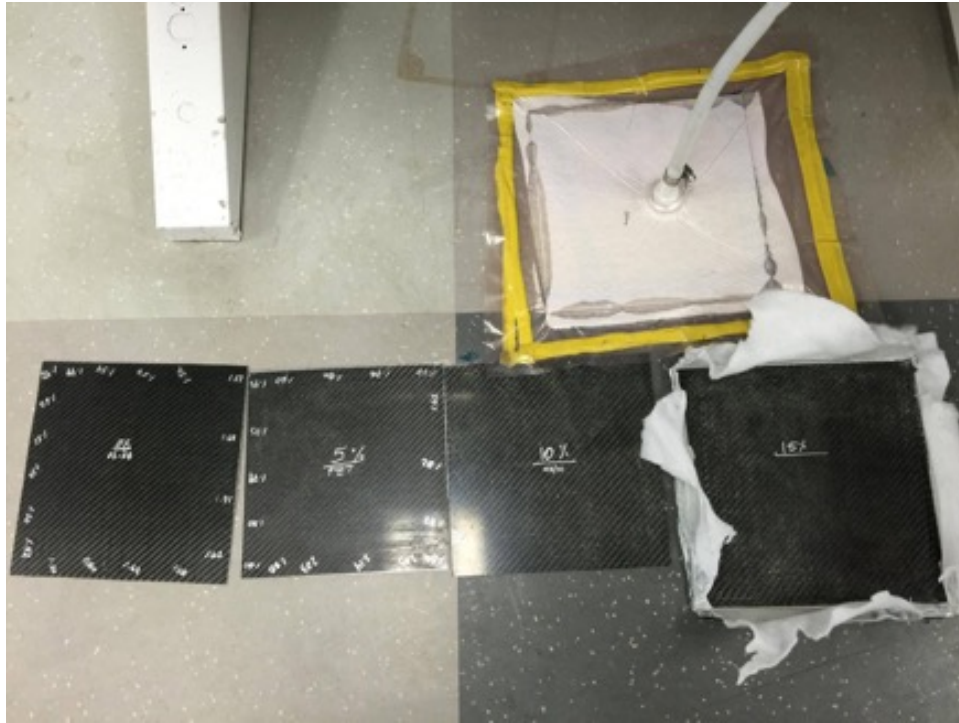


Figure 2.2: Variations on PZT wt.%



Figure 2.3: Glove Box

The composite matrix constituent phase consists of an epoxy named System 2000 from the company Fiberglast. System 2000 epoxy acts as the main component of the composite matrix 2.4; it contains a medium viscosity that is lower compared to others. This light amber epoxy used for fabricating high strength parts as well as demanding structural applications is considered to be the highest ultimate strength epoxy for room temperature applications. It is also recognized for the convenient handle it has and maximization of physical fiber properties. The epoxy must react with another substance to generate a solid material; this material is called a hardener. The function of the hardener is to act as a catalyst for the epoxy and solidify it, for this reason, the hardener 2020 from Fiberglast was selected and applied 2.4. This hardener has a 20-minute curing time, and the ratio between the epoxy and the hardener is a four to one (4:1) by volume. This curing time must be taken into account while manually transferring/brushing the epoxy onto the woven carbon and glass fiber laminas.



Figure 2.4: Fiberglass System 2000Resin and 2020 Hardener

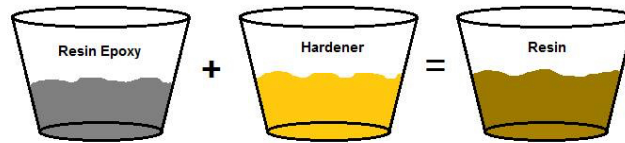


Figure 2.5: Epoxy Schematic

The combined matrix epoxy is mechanical stirred until completely mixed, the temperature it rises to and the time are critical parameters that must be monitored. The mixture is then manually hand brushed onto each layer using a regular paint brush. Lamina order must be ready and taken into consideration, a task that must be remembered is that once the first lamina is brushed, it must be flipped it for it to receive full cover. Once the resin has covered the nine layers, the entire composite is then placed between two prepared aluminum plates to commence the modified autoclave vacuum bag composite molding process. The vacuum bag procedure consists of several materials that must follow a sequence to achieve a successful composite laminate. This procedure is graphically represented on 2.6. The first layer consists of a vacuum bag film with the perimeter of the entire laminate covered with sealing tape, this being the outermost top layer of the bag provides the airtight seal that allows vacuum to increase and actuate pressure on the laminate. The following material is a breather and bleeder film that traps any excess epoxy/PZT combination that escapes from the Interlaminar region. Subsequently, the mold for the composite being the two aluminum

plate, these are covered by a release film that eases the separation between the plate and the composite by repelling excess epoxy. That order repeated symmetrically for the bottom. The vacuum compressing the plates forces the excess matrix to exit by all four sides; this visually ensures that the matrix has gone through the entire composite contour. Once the bag experiences vacuum, the gauge starts to indicate pressure the desired range is 60 to 80 KPa, in the case of lower pressure, the air seal tape must be repressed to close any existing gaps. The bag will remain unchanged for the following 24 hours this will allow the epoxy to cure.

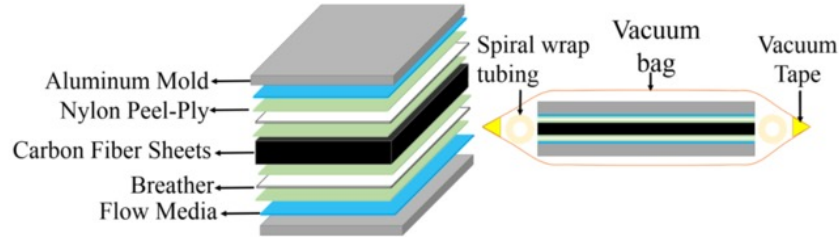


Figure 2.6: Vacuum Bag Layers and Material

Afterward, the separation of the plates is done manually with conventional lab tools. The composite plate is then sectioned off into different sample sizes with a silver marker 2.7. The reason behind the multiple size sections is the ASTM (American Society for Testing and Materials) requirements for each of the tests that will be applied. For this thesis, four samples were selected for the pyroelectric test and twenty for the three-point bending tests. The cuts were made manually and locally with a modified tile cutter 2.9.





Figure 2.7: CFRP Sectioned plate



Figure 2.8: CFRP Cut Cross section

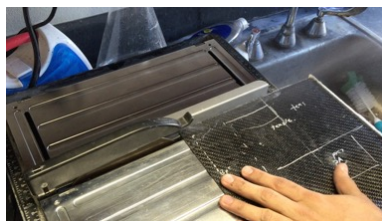


Figure 2.9: Modified Tile Cutter

## Chapter 3

### Methodology and Instrumentation

Since multifunctional composites are and will become a big part of engineering project and structures, behavioral characterization must be performed. The approach to accomplish this task on carbon/glass fiber reinforced plastic composites is of several methods and techniques. In continuance the thesis will describe each one individually, these are mechanical, electrical and sensory tests under temperature or load changes.

**Mechanical Tests:** The mechanical properties were analyzed this includes strength, stiffness, bending modulus and toughness. The method used to obtain these characteristics of the CFRP composites was using "Three Point Bending" tests following the appropriate ASTM standard. The volume fraction and density values also from part the mechanical properties obtained, these have been achieved via another ASTM standard.

**Electrical:** The ability of the LCR meter to measure impedance and capacitance for the CFRP allowed the characterization of structural health monitoring (SHM).

**Composite Composition:** Each of the CFRP composites varied slightly due to the manual manufacturing process they undergo therefore Scanning electrode microscopy (SEM) and digital microscopy needed to be performed on them. These instruments permitted accurate measurement of the electrode/dielectric material thickness.

**Sensor Performance:** A collaboration between a Picoammeter and a computer data acquisition system on a computer allowed the recording of signal response due to piezoelectric and pyroelectric properties of the composites. This signal can be used for temperature calculation and energy harvesting approximation.

In continuance each of the procedures will be explained in detail.



### 3.1 Dispersion

The dispersion of the ceramic piezoelectric spheres, 840 PZT powder, is a crucial variable that cannot be controlled due to the used manufacturing procedure. The method used to disperse the powder was done by mechanical stirring as well as sonication baths which are vibration energy sound waves, but due to the fast curing time of the epoxy, this was limited.

### 3.2 Three Point Bending Tests

The approximation of the CFRP bending modulus, strength and fracture toughness on flexural condition were obtained following ASTM standard 799. The samples satisfied the standard by having a span-thickness ratio of 32:1; with a used crosshead velocity of 1 mm/min. The test is done by placing the test sample between two support points and applying the desired load on the midway section shown on 3.1. The load was applying by an Instron 8801 Fatigue system in the Challenger-Columbia laboratory at The University of Texas at El Paso 3.2.

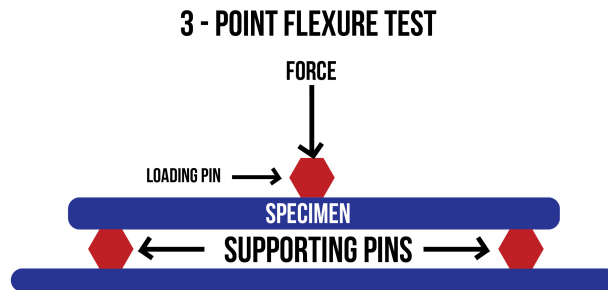


Figure 3.1: Three Point Bending Schematic



Figure 3.2: Instron 8801 Machine

The maximum strain at the outer surface occurs at the mid-span, equation 3.1 is used to calculate it.

$$\epsilon_{3pt} = \frac{6\delta h}{L^2} \quad (3.1)$$

Where ( $\epsilon_{3pt}$ ) is the maximum strain, ( $\delta$ ) is the mid-span deflection, ( $h$ ) is the thickness of the beam and ( $L$ ) is support span.

Equation 3.2 is used for the stress at any point on the load-deflection curve.

$$\sigma_{3pt} = \frac{3PL}{2bh^2} \quad (3.2)$$

Where  $P$  is the applied force,  $b$  is the width of the beam and ( $\sigma_{3pt}$ ) is the stress at the outer surface that also occurs in the load span region.

The equation (3.3) is used for the flexural modulus of elasticity which is the ratio of stress to a matching strain at any given point in the stress-strain curve for orthotropic composites.

$$E_f^{secant} = \frac{L^3 m}{4bh^3} \quad (3.3)$$

Where  $(E_f)$  is the flexural secant modulus of elasticity and  $(m)$  is the slope of the secant of the force-deflection curve.

Equation (3.4) is used for fracture toughness also knows that the absorbed energy, the principle is to integrate the area under the stress-strain curve per volume and thickness.

$$Energy = \int_0^{\delta_f} \frac{P \cdot d\delta}{bh^2L} \quad (3.4)$$

### 3.3 Constituent Volume fractions and Density Calculations

In composites area, an important characterization factor is the fiber volume fraction as well as the overall composite density. The executed ASTM standards were D792-00 for density and D2584-02 for the fiber volume ratios.

#### 3.3.1 Density

The composite Density procedure consists of the following steps:

Weight the composite sample on dry conditions.

Attach a wire to the sample and fully submerge into a measured distilled water container. The wire submersion point must be marked for step 3 and test repeat-ability.

Weight the wire by itself by also submerging it into distilled water to the marked point.

The following equation(3.6) is used to determine the composite density.

$$\rho = \frac{a}{a + w - b}(0.9975) \quad (3.5)$$

Where  $(a)$  is the composite sample's dry weight,  $(b)$  is the combined wet weight of the sample and wire and  $(w)$  is the approximate weight of the wire. The values of .9975 come from the distilled water density which is .9975 gr/cm<sup>3</sup> at 23 C (considered room temperature)

#### 3.3.2 Volume Fraction

Several methods are in existence for the determination of the constituent volume fractions; optical analysis of the transverse cross-sectional area, acid digestion, the burnout method (CITE) and gravitational method.

For the CFRP composites that have a porosity level of less than 1%, the volume ratio can be directly obtained from the constituent parts and a gravimetric relationship in equation (3.6)

$$V_f = \frac{\rho_c - \rho_m}{\rho_f - \rho_m} \quad (3.6)$$

Where the  $c$ ,  $m$ , and  $m$  correspond to fiber, matrix, and composite, respectively.

The alternative is the burnout method, where the composite sample is placed into a crucible and exposed to a temperature higher than 400 C where carbon fiber vaporizes, via a controlled and programmable furnace. This approach consists of weighing a sample then temperature exposing it in a furnace until the carbon and matrix are dissipated. A cleansing distilled water bath is then performed to wash out the ashes from the residue. After the rinse, the samples are dried and weight again. Equation (3.7) then gives the volume fraction.

$$V_f = \frac{W_f/\rho_f}{W_c/\rho_c} \quad (3.7)$$

where  $W_F$ , and  $W_c$ , are the weight of the composite and fibers, respectively.

As for the optical analysis, a SEM machine is utilized to calculate the tow volume fraction, this si done by digitalizing the image into pixels and then determining the surface area of matrix and fiber.

### 3.4 SEM and Digital Microscope

The combination of a scanning electron microscopy machine with a digital microscope is utilized for imaging analysis for thickness determination, ceramic sphere particle dispersion, and CFRP composite defects (cross-sectional voids and surface epoxy voids) 3.3 3.4.



Figure 3.3: Hitachi TM-1000 Tabletop Microscope

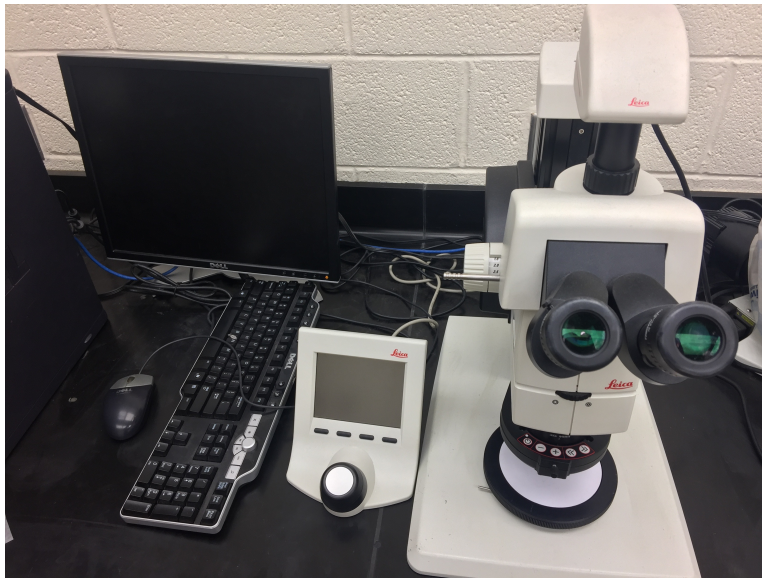


Figure 3.4: Digital Microscope

### 3.5 LCR Meter

The LCR (Inductance, Capacitance and Resistance) meter is an HP 4284A meter at 1 Vrms with the parallel equivalent circuit set up that has a frequency range from 100 Hertz to 1 MHz. The machine is connected to LabView which is a programming application that allows an automated and systematical recording of data. The image of the used LCR meter is 3.5 in the Challenger-Colombia laboratory at The University of Texas at El Paso.



Figure 3.5: LCR Meter

#### 3.5.1 Natural Frequency

The adequate scanning frequencies for impedance depends on the first natural frequency. Therefore the natural frequency of the samples must be known. The selected samples were of 6 inches in length and 1 inch in width. This size was chosen to replicate a cantilever beam principle; the surface was hand sanded as well as the beginning of the beam where the electrodes were placed, and the sample clamped. 3.6 shows the set up for the cantilever beam and equation 3.8 is the cantilever beam principle.

$$\frac{d^2}{dx^2} \left\{ EI(x) \frac{d^2 Y(x)}{dx^2} \right\} = \omega^2 m(x) Y(x) \quad (3.8)$$

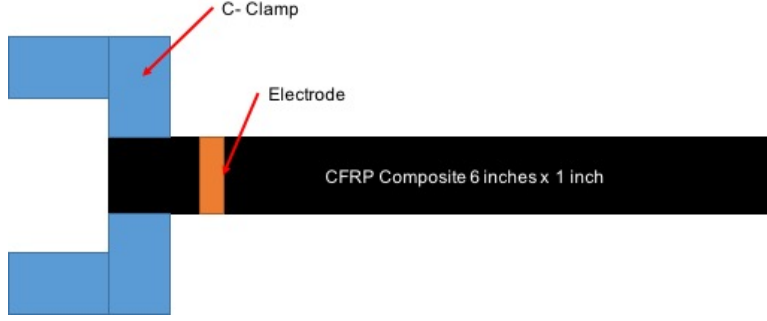


Figure 3.6: CFRP Composite Cantilever Beam Set Up for SHM

The equation(3.9) is used for cantilever's moment of inertia.

$$I = \frac{bd^3}{12} \quad (3.9)$$

Where  $I$  is the moment of inertia,  $b$  is the width, and  $d$  is the diameter of the cross section for a rectangular cross section.

Afterward equation 3.10 is used to calculate the undamped first natural frequency of a beam.

$$\omega_1 = 1.875^2 \sqrt{\frac{EI}{\rho AL^4}} \quad (3.10)$$

Where  $E$  is the modulus of rigidity of beam material,  $I$  is the moment of inertia of the beam cross-section  $\rho$  is the material density and  $L$  is the beam length.

By having the determination of the natural frequency, the LCR meters frequency sweep range is set at steps of 10 Hertz then the LabView program is ran. The results are the impedance vs. frequency plot. That becomes the original impedance the unchanged samples has, following that test an aluminum block is placed at the utmost extremity of the cantilever beam. The block produces internal stresses, and as a second test runs a noticeable change in the impedance vs. frequency, the plot is detected. This shift is the principle the thesis utilized for the application of CFRP Composites for Structural Health Monitoring.

## 3.6 Signal Response Set Ups

### 3.6.1 Piezoelectric and Pyroelectric

The 840 PZT powder ceramic sphere particles used on the CFRP allows for two effects to come into play: Piezoelectric and Pyroelectric. Both effects are utilized in this thesis; the piezoelectric effect focused on the energy harvesting side, and the Pyroelectric is used for both the energy harvesting and temperature sensing aspects.

### 3.6.2 Piezoelectric Effect

For this tests, the CFRP are set in a compression-compression Instron machine 3.2. As the load is applied to the crystals in the PZT powder are strained creating the "dipole movement" that unbalances the electric charge within the structure and therefore a sudden voltage generation is observed. The machine was set for a compression-compression with a 5 Hz loading frequency ranging from 7 Kn to 14 Kn, to the varying wt.% of the composites. After the test the application of equation 3.11 was used to find the capacitance and obtain the effective piezoelectric coefficients.

$$|d_{33}|_{design} = \frac{\Delta V \cdot C}{\Delta F} \quad (3.11)$$

where  $\delta V$  is the voltage range response of the compression-compression test,  $\delta F$  is the force range response, and  $C$  is the capacitance measure in Farads this follows the equations from the constitutive equations on chapter 1.

$$D_i = d_{i\mu} \cdot T_\mu \quad (3.12)$$

where  $D_i$  is charge density ( $CV/Area$ ),  $d_{i\mu}$  is the piezoelectric coefficient matrix and  $T_\mu$  is the stress tensor.



### 3.6.3 Pyroelectric

#### Energy Harvesting - Charge

The theory for this test is similar to the piezoelectric effect, straining the crystals inside the PZT powders, but instead of it being via an applied load it is done by cyclic changes in temperature. A hand heat gun 3.8 provides heating and cooling air which are then applied to the test specimen. The position was fixed at a distance of 10 cm from the CFRP composite surface. By utilizing the current response from the composite equation 3.13 was applied to calculate the charge generated in the varying wt.% samples. This charge can later be utilized to charge or extend battery life of low energy consumption devices.

$$Q = \int_{t_0}^{t_f} I dt \quad (3.13)$$



Figure 3.7: Hand held Heat Gun for Pyroelectric test

#### Temperature Sensor

The theory for this test is similar to the piezoelectric effect, straining the crystals inside the PZT powders and therefore unbalancing the internal charge in the structure. The current is generated by the "dipole movement" through the change of polarization, the charge effect then leaks that is why the equation mentions a change in temperature with respect to time. The difference is that instead of it being via an applied load it is done by cyclic changes in temperature.

There were several heating elements experimented throughout this thesis. The heating elements were: Hotplate 3.9, Silicon heating pad 3.10, Heat gun 3.8 and a Tube Furnace 3.11.



Figure 3.8: Hand held Heat Gun for Pyroelectric test



Figure 3.9: Hotplate for Pyroelectric setup



Figure 3.10: Silicone Rubber Heating pad for Pyroelectric setup



Figure 3.11: Controlled Tube Furnace for Pyroelectric setup

The heating elements provided heating and natural/forced cooling of the sample through convection. The samples generated a current response which can then be utilized as a temperature sensor. The way this setup is established is by having the electrodes of the samples attached to a Picoammeter to detect the changes in current generated from the sample. The sample is placed inside/on top of whichever is the selected heating element to give the specimen a change in temperature with respect to time. The heat gun provides a high change of temperature but is unstable whereas the tube furnace has a more stable heating and cooling environment.

The generated current is then utilized on the pyroelectric equation 3.14.

$$I = \frac{dQ}{dt} = -pA \frac{dT}{dt} \quad (3.14)$$

where "I" is current, "T" is temperature, "t" is time, "Q" is the generated charge, "A" is the surface area of the electrodes, "dT/dt" is the rate of temperature change and "p" is the pyroelectric coefficient of the material.

Equation 3.14 can be rewritten as equation 3.15 to back-calculate the temperature of the pyroelectric PZT powder at any time considering initial room temperature.

$$T_f = -\frac{1}{pA} \int_{t_i}^{t_f} I dt + T_i \quad (3.15)$$

Here, (Ti) is the initial temperature of the pyroelectric ceramic powder at the time (ti),

this is considered to be room temperature. ( $T_f$ ) is the final temperature of the material at any time ( $t_f$ ). By measuring the initial temperature, pyroelectric coefficient, electrode area and total current generated from the heating and cooling at a certain time, the temperature can be calculated.

## Chapter 4

### Results

#### 4.1 Mechanical Characterization Results

##### 4.1.1 Density

Following ASTM 792 shown in the methodology section, the displayed volume of the carbon fiber reinforced plastic composite are shown in 4.1. The multiplication of the distilled water density is of .9975 g/cm<sup>3</sup>. The initially obtained density was 2.9 g/cm<sup>3</sup> for the 0 wt.% composite, with the addition of PZT particles this increased until the 10wt.%. Afterward, a noticeable decrease occurred, due to the augmentation of epoxy voids and imperfections during curing. These given results are in the usual range for the type and style setup. It was noticed that the increase of PZT particles in the epoxy mixture caused a temperature rise in the mechanical stirring, this change accelerated the curing process.

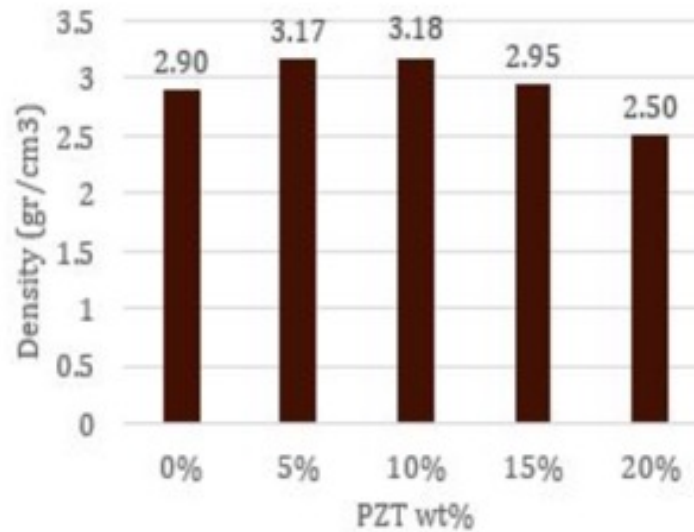


Figure 4.1: CFRP Composite Density

#### 4.1.2 Volume Fraction

The volume fraction was calculated following the mentioned procedure in the methodology section. The results also are shown on 4.2 graphically demonstrate a reduction in fiber volume which was expected, as more PZT particles start taking an increased volume percentage. The given results from the 0-15 wt.% show very high volume fraction that differs from published literature reviewers.

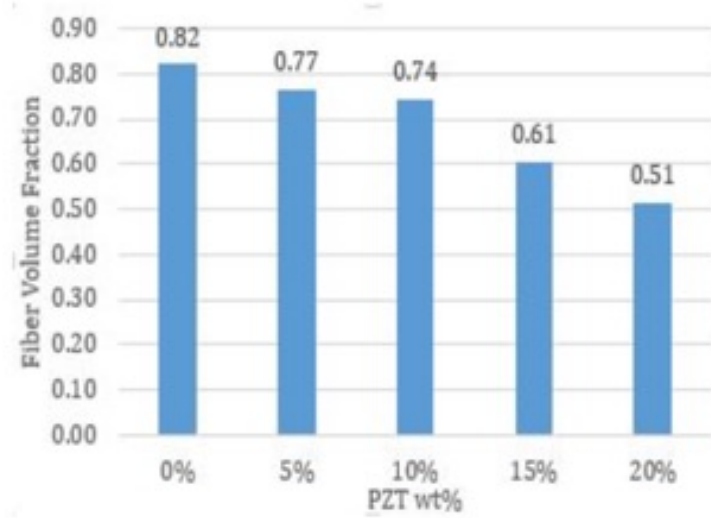


Figure 4.2: CFRP Composite Fiber Volume Fraction

#### 4.1.3 Dispersion Analysis

Surface and thickness analysis was made of the CFRP composites via a digital microscope and scanning electron microscope. The results show that with an increase of PZT particles, the agglomerates become more substantial in the depressions between the fill and warp fibers. These agglomerates directly affect the result variation between each sample and varying wt.%. Therefore in the future works section a proposed idea to increase the dispersion efficiency, control and quality during manufacturing. The mentioned surface dispersion for the varying wt.% can be seen in 4.3 ; 4.4 the glass fiber thicknesses are observed.

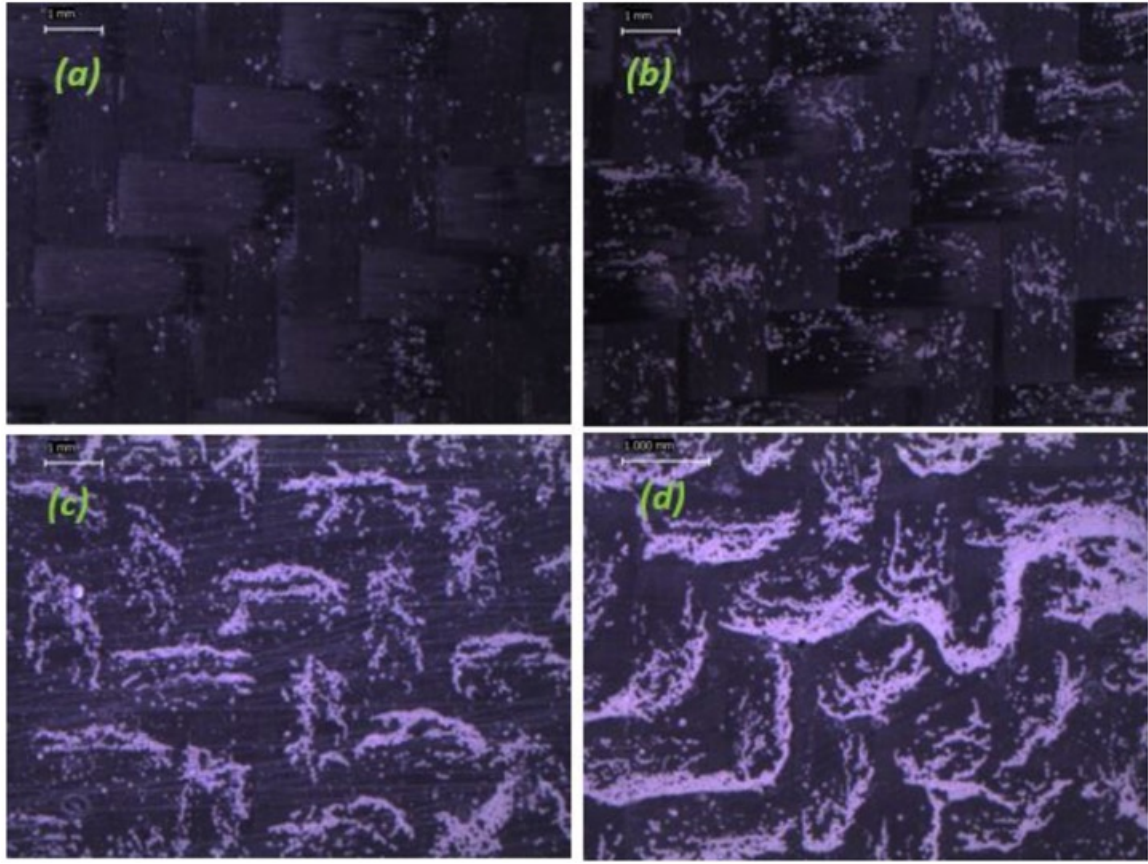


Figure 4.3: CFRP Composite Surface Dispersion

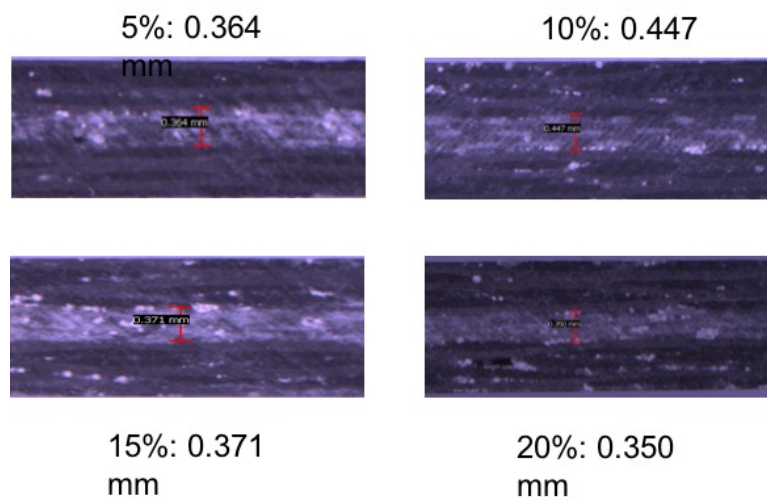


Figure 4.4: CFRP Composite Cross Sectional View

#### 4.1.4 Three Point Bending Results

Following ASTM D790-02 for flexural mechanical properties of composites shown in the three-point bending sections of methodology. The given properties that can variate from this test are directly proportionate to the samples depth, temperature, and atmospheric conditions. The overall sample width was off  $12.49 \pm .0233$  mm with an overall thickness of  $2.2022 \pm .0205$  mm the deviation between the samples were of .1% and .95% for each one respectively. The initial set amount of samples between each variation was of 20, but each wt.% had some faulty ones that were dished out. That being said a minimum of 18 samples were used and MATLAB was utilized for processing the data.

In 4.5 the results of the three-point bending tests are shown. The maximum mechanical strength was found in the 0 wt.%; this was expected. It was expected due to the published literature reviews showing and stating that the addition of a sensing capability is at the cost of mechanical property decay. These results demonstrate the relationship between the decay and addition of PZT. The region between 10 wt.% and 15 wt.% shows the decrease in properties. The Young's modulus follows a similar trend and also increases slightly in the 20 wt.% samples.

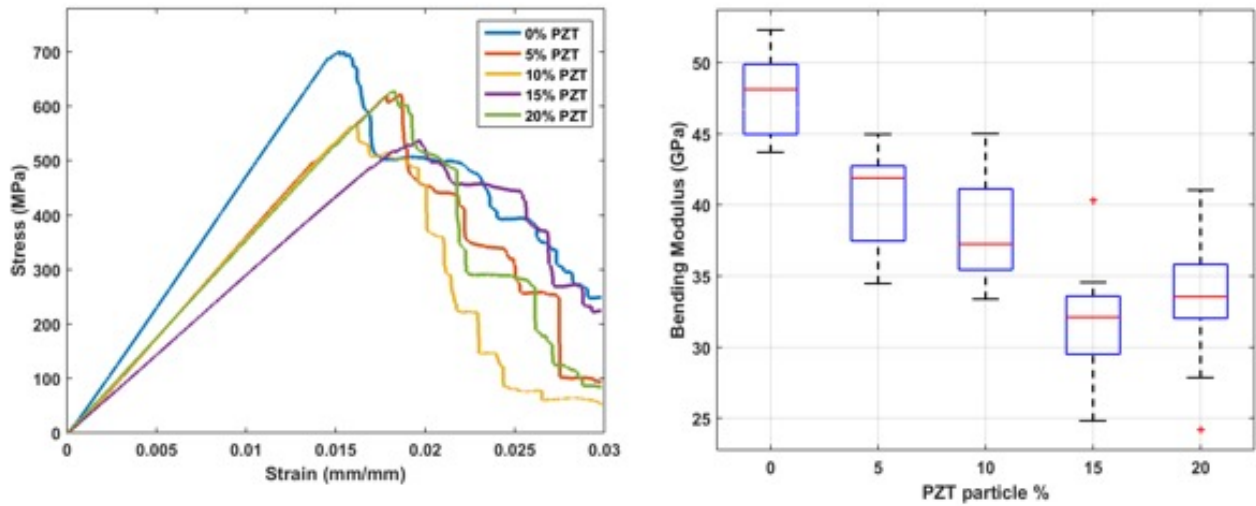


Figure 4.5: Stress-Strain Curve and Bending Modulus

On 4.6 the strength and strain were obtained, the strength follows the same pattern



where with an increase of PZT particle concentration a mechanical property decrease follows, and seems to even out between the 15 wt.% and 20 wt.%. However, for the strain, it appears to improve with the addition of PZT particles slightly but not sought where the composite first yield changes. The overall decay from 0 wt.% to 20 wt.% is of 30% from 400 MPa to 250 MPa.

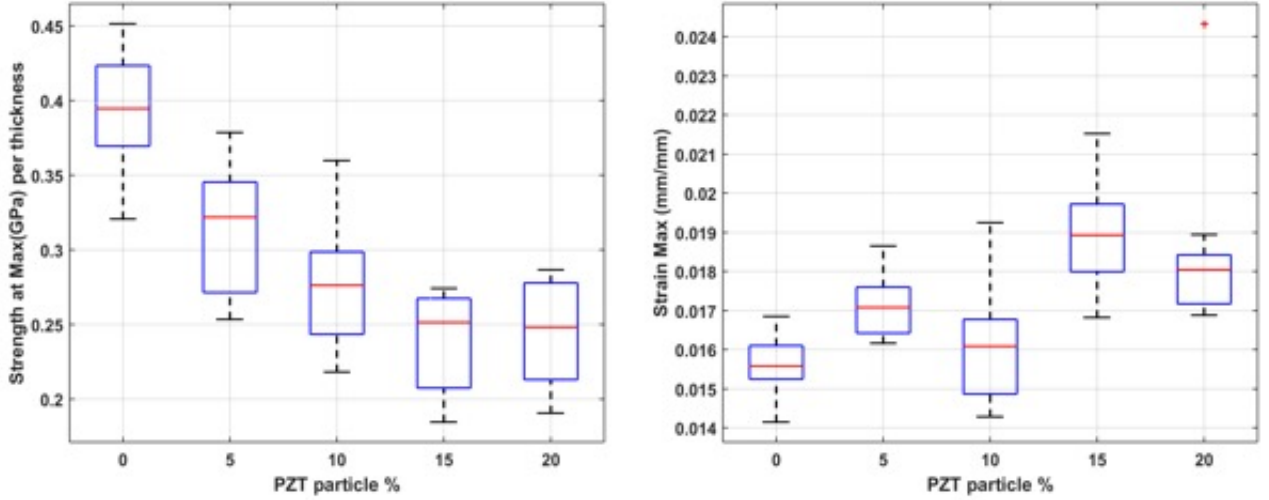


Figure 4.6: CFRP Composite Maximum Strength (Left) and Strain at that point (Right)

Analysis of the total energy absorbed was also plotted in 4.7. The energy continues the pattern of decay as PZT particles are added. The trend seems to stabilize after reaching the 10 wt.%. The reasoning behind this stabilization is shown in the overall decrease from volume fractions including the increased voids and interfacial interactions.

## 4.2 Electrical Characterization Results

The utilization of PZT materials has been researched extensively before, however, the use of only PZT particles as a reinforcer and sensing capability enabler has not. For SHM PZT particles have been used on top of a PZT plate as an enhancer and as for temperature sensors, no research was found. The following section will have the different applications this thesis performed:

- 1: Piezoelectric effect for energy harvesting
- 2: Piezoelectric effect for SHM.
- 3: Pyroelectric effect for temperature sensors
- 4: Pyroelectric effect for energy harvesting

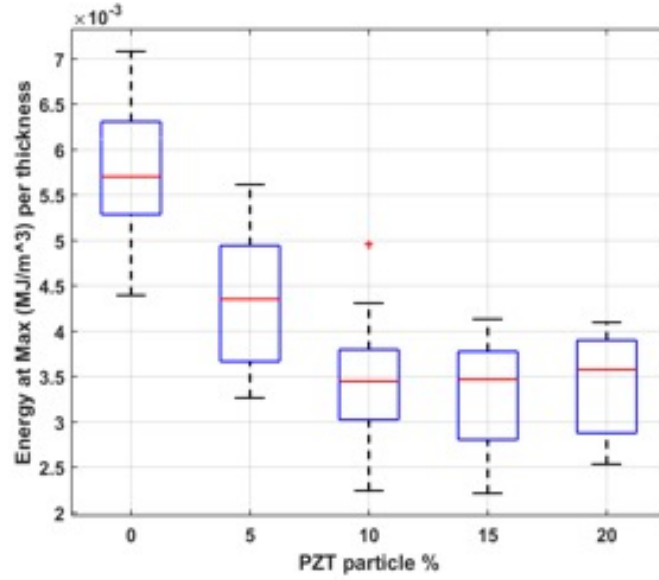


Figure 4.7: CFRP Composite Toughness (Area under the Load-Displacement Curve)

#### 4.2.1 Piezoelectric Effect for Energy Harvesting

##### Piezoelectric Constant

The compression-compression testing on methodology was applied on the recently cut composite samples; the results bared no response therefore they were subjected to the polling procedure also in the methodology. They were poled for 1 hour with a range of 1-1.5 kV.

The low response con is attributed that the PZT particles act as enhancers only in the dielectric material i.e. the glass fiber. Due to this fact, a section in future work was added to have the full wt.% concentration in that area.

The results were obtained via a 5 Hz loading frequency cycling from 7 kN to 14 Kn. The capacitance was utilized to calculate the effective piezoelectric coefficient. The results are: .40, .47, .51, and .58 fC/N for 5 wt.%, 10wt.%, 15wt.% and 20wt.% respectively. Shown in 4.8.

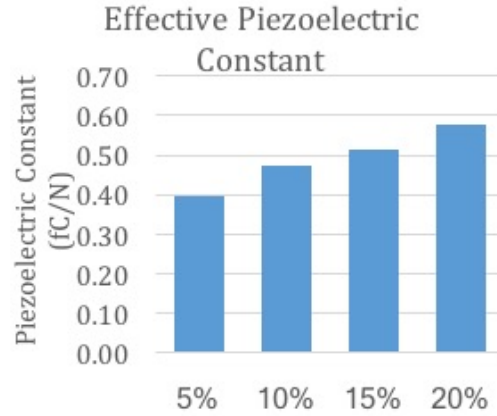


Figure 4.8: CFRP Composite Piezoelectric Constant

#### 4.2.2 Piezoelectric for Structural Health Monitoring

The use of an LCR meter to measure the impedance of a 6X1 composite in a cantilever beam configuration bared the following results. The use of PZT particles can be utilized as effective SHM composite enhancers.

The following plots 4.9 and 4.10 will show the response of with and without the block at the end of the beam, the range is then compared. For the 0 wt.% the range is between 100-200 Ohms 4.9 and for 20 wt.% is around 15 E6 Ohms 4.10.

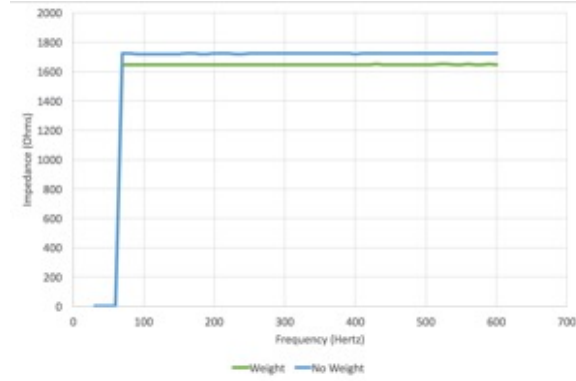


Figure 4.9: CFRP Composite SHM for 0 wt.%

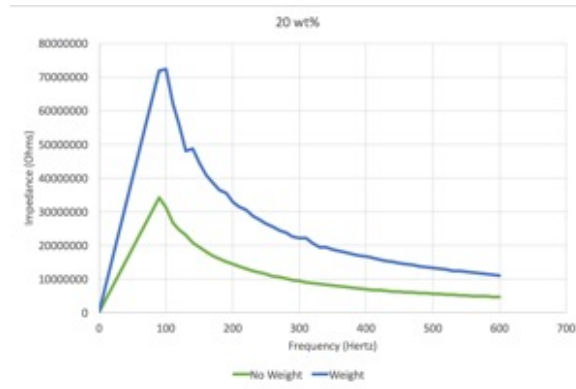


Figure 4.10: CFRP Composite SHM for 20 wt.%

### 4.2.3 Pyroelectric for Energy Harvesting - Charge Generated

With the utilization of a heat gun these were the following results for the charge generated shown in 4.11. A minimum of 3 samples sets were subjected to 5 heating and cooling cycles and repeatedly tested. The test lasted 4 minutes per cycle, and the range of charge is from .5  $\mu\text{C}$  to 4.8  $\mu\text{C}$  for a surface area of 6.45  $\text{cm}^2$ .

### 4.2.4 Pyroelectric for Temperature Sensing

For this test, the CFRP are utilized as temperature sensors by back calculating the composite temperature by characterizing the generated current. A test guideline was made by using a PZT ceramic plate 4.12; once this composite tested feasible the addition of PZT

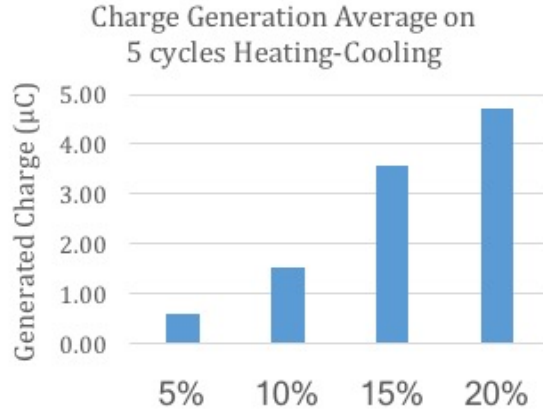


Figure 4.11: CFRP Composite Charge under Temperature Cycles

particles came into play. These tests were done with the Silicone pad as the heating agent. The test with the PZT plate gave a response of 13 Nanoamps with the 20 wt.% CFRP giving a response of 3.4 Nanoamps 4.13.

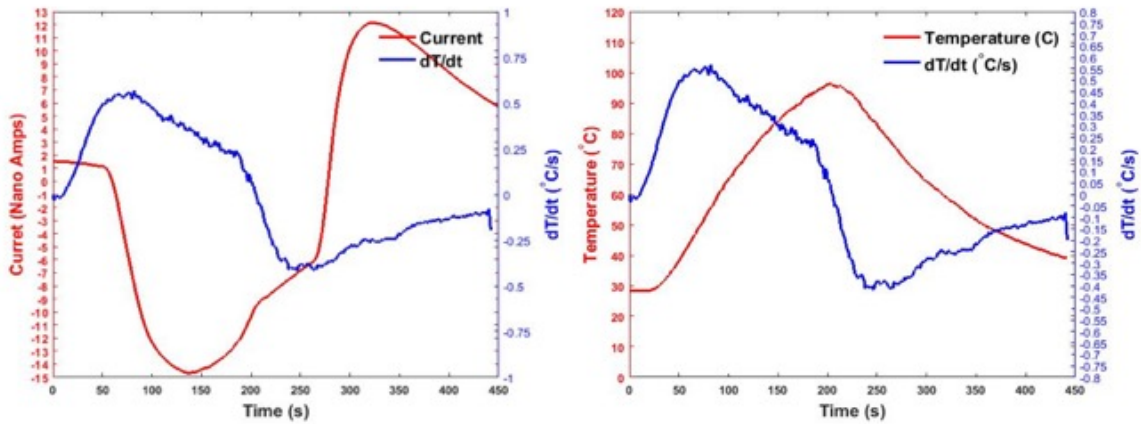


Figure 4.12: CFRP Composite PZT Plate Response

When using the output current from the 20 wt.% sample to calculate temperature and comparing it to the thermocouple temperature a deviation can be seen 4.14. This is due to not having an adequate pyroelectric coefficient for the composite; therefore under future work further testing needs to be made. An example made was multiplying the commercial pyroelectric factor by 20% for the 20wt.% composite to have a nice matching curve as seen on 4.15.

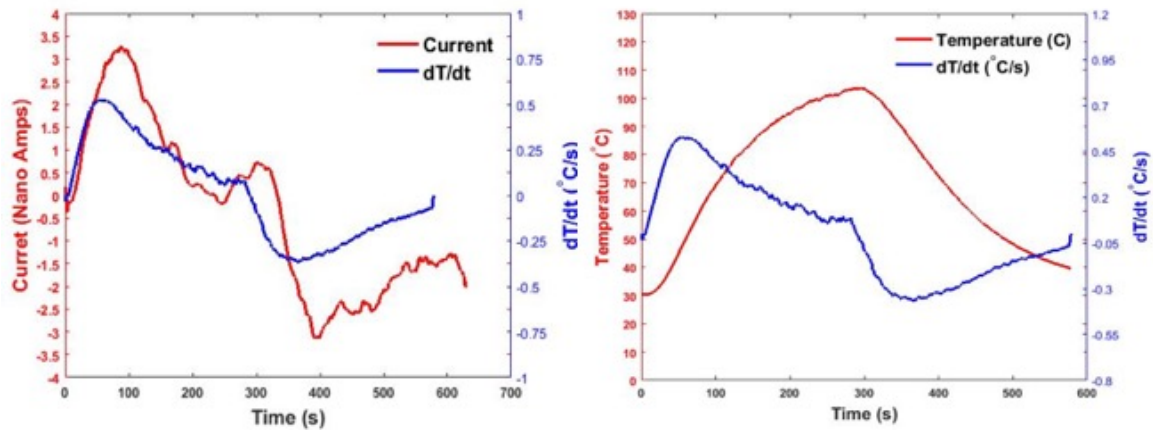


Figure 4.13: CFRP Composite 10 wt.% Response

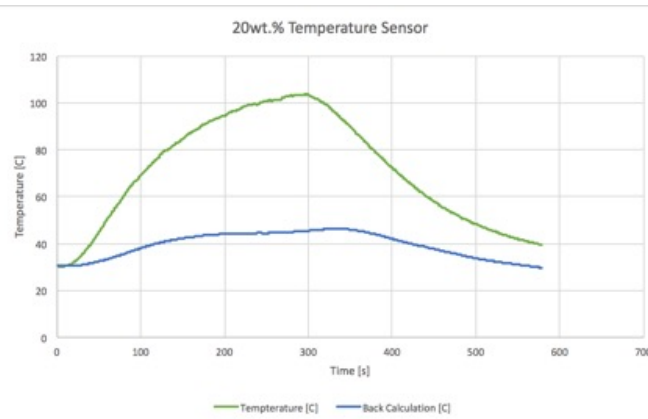


Figure 4.14: CFRP Composite 20 wt.% Temperature Calculation

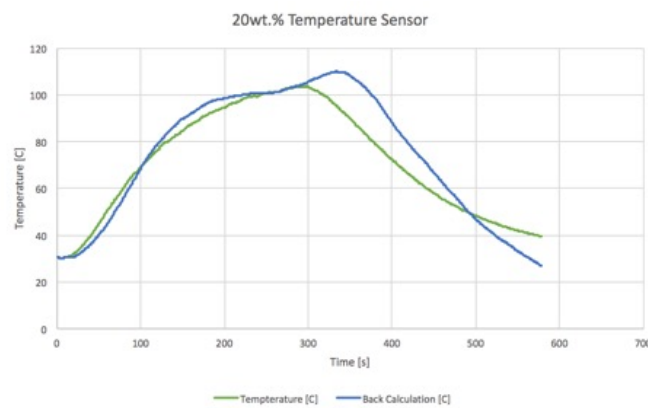


Figure 4.15: CFRP Composite 20 wt.% Temperature Calculation

Due to some variations in testing the heating element was changed to a tube furnace where the heating and cooling would be better controlled. The four 15 wt.% samples were tested were two were poled and two non-poled.

One poled sample generated 3.5 Nanoamps 4.16 while the other generated 2.5 Nanoamps 4.17, in comparison to the non-poled samples that generated .4 Nanoamps 4.18 and .2 Nanoamps 4.19 this was expected as the polling procedure enhances the pyroelectric effect.

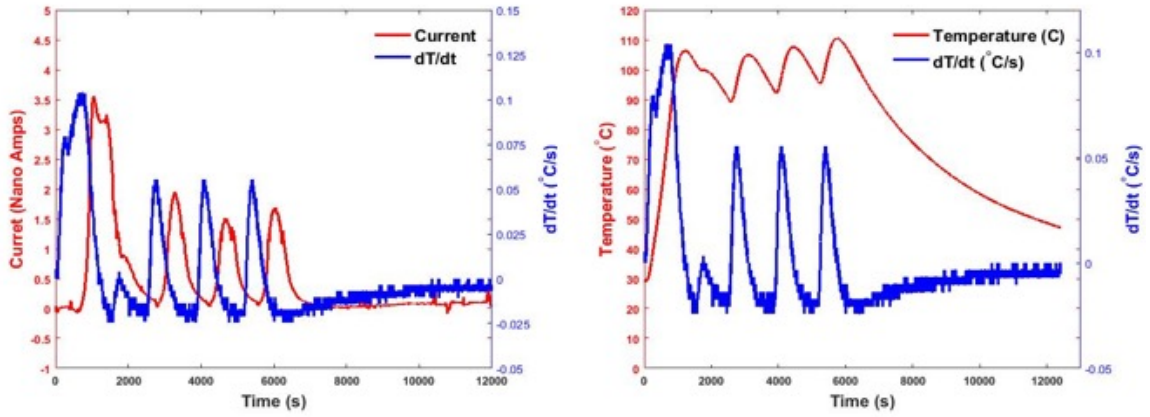


Figure 4.16: CFRP Composite Poled Sample 1 Tubefurnace Test Data

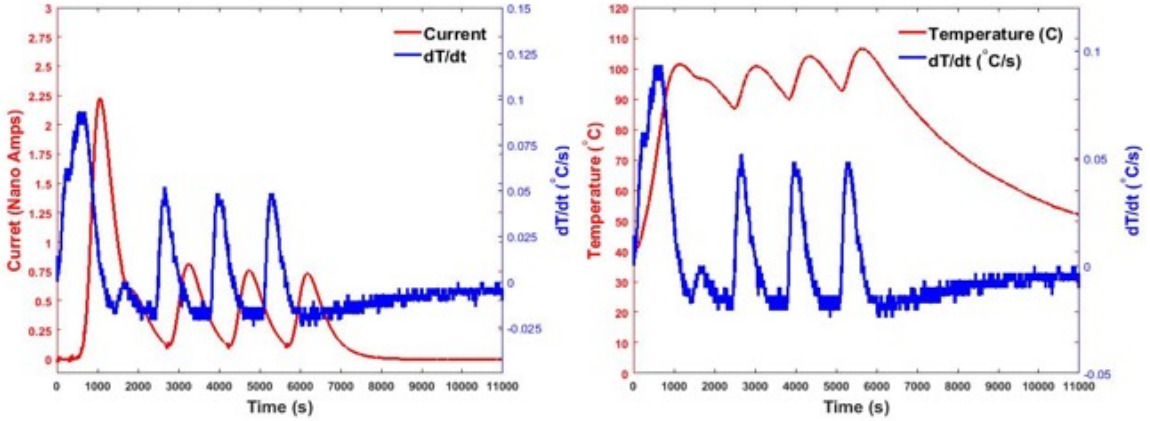


Figure 4.17: CFRP Composite Poled Sample 2 Tubefurnace Test Data

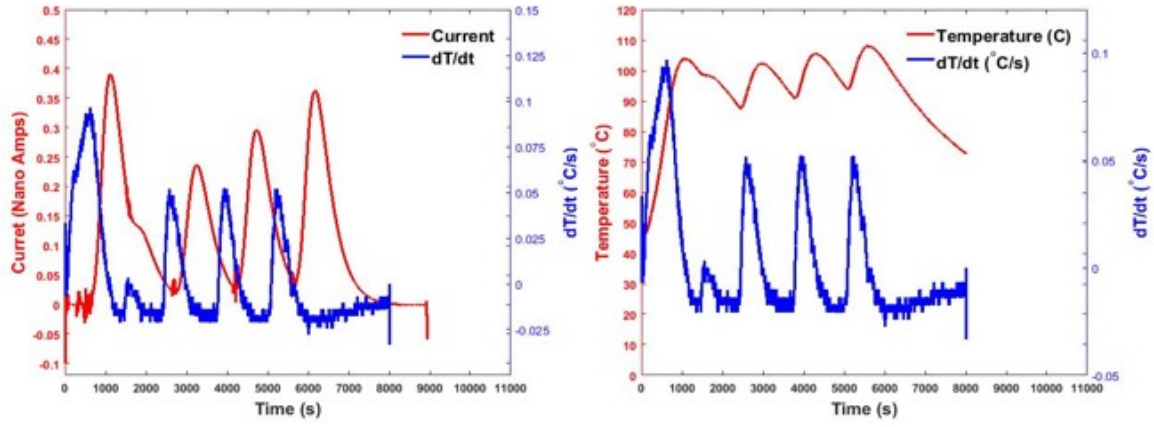


Figure 4.18: CFRP Composite Non-Poled Sample 1 Tubefurnace Test Data

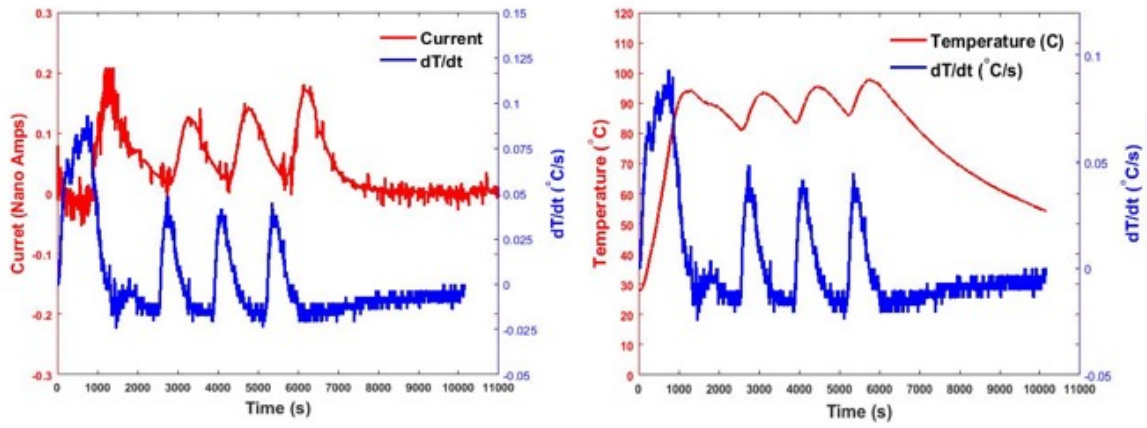


Figure 4.19: CFRP Composite Non-Poled Sample 2 Tubefurnace Test Data



## Chapter 5

### Conclusion and Future Work

As this thesis concludes the application of CFRP composites with 840 PZT powder particles is feasible, the several applications that were tested can be improved and here are some of the possible actions to take. The impact of the research in this study is of high value. Therefore future work has been throughout, that The University of Texas at El Paso might continue to develop. One of the main things to add is quality control to the manufacturing process, and by this, I mean the dispersion of the 840 PZT powder particles in the CFRP composite. A way to increase a better dispersion is by utilizing a spray gun this would eliminate the possible agglomerations the composites have therefore reducing result deviations. As the 840 PZT powder, is used as a response enhancer if the spreading would concentrate only on the dielectric material layers (glass fiber) the enhancement would be higher. Once these higher results bare the pyroelectric coefficient must be studied to have an accurate temperature calculation, additionally for structural health monitoring the response analysis must be explored to better understand the damage progression by seeing impedance peak shifts. The study of elastic and fracture mechanics of the CFRP composite must also be studies.

## References

- [1] Suresh G Advani and Kuang-Ting Hsiao. *Manufacturing techniques for polymer matrix composites (PMCs)*. Elsevier, 2012.
- [2] Pulickel M Ajayan, Linda S Schadler, and Paul V Braun. *Nanocomposite science and technology*. John Wiley & Sons, 2006.
- [3] Cesim Atas and Onur Sayman. An overall view on impact response of woven fabric composite plates. *Composite Structures*, 82(3):336 – 345, 2008.
- [4] E.J. Barbero. *Introduction to Composite Materials Design, Second Edition*. Composite Materials. Taylor & Francis, 2010.
- [5] S. Bose and A. Bandyopadhyay. *Characterization of Biomaterials: Chapter 1. Introduction to Biomaterials*. Elsevier Science, 2013.
- [6] Walter Guyton Cady. *Piezoelectricity: An introduction to the theory and application of electromechanical phenomena in crystals*. McGraw-Hill, 1946.
- [7] Tsu-Wei Chou. *Microstructural design of fiber composites*. Cambridge University Press, 2005.
- [8] Isaac M Daniel, Ori Ishai, Issac M Daniel, and Ishai Daniel. *Engineering mechanics of composite materials*, volume 3. Oxford university press New York, 1994.
- [9] D. Ding. 2 - processing, properties and applications of ceramic matrix composites, sicf/sic: an overview. In I.M. Low, editor, *Advances in Ceramic Matrix Composites*, pages 9 – 26. Woodhead Publishing, 2014.
- [10] Lorna J Gibson and Michael F Ashby. *Cellular solids: structure and properties*. Cambridge university press, 1999.
- [11] Yiping Guo, Kenichi Kakimoto, and Hitoshi Osato. Phase transitional behavior and piezoelectric properties of. *Applied physics letters*, 85(18):4121–4123, 2004.

- [12] Suong V Hoa. *Principles of the manufacturing of composite materials*. DEStech Publications, Inc, 2009.
- [13] D. Hull and T.W. Clyne. *An Introduction to Composite Materials*. Cambridge Solid State Science Series. Cambridge University Press, 1996.
- [14] Hae Jin Hwang, Toru Nagai, Tatsuki Ohji, Mutsuo Sando, Motohiro Toriyama, and Koichi Niihara. Curie temperature anomaly in lead zirconate titanate/silver composites. *Journal of the American Ceramic Society*, 81(3):709–712, 1998.
- [15] Michael W Hyer. *Stress analysis of fiber-reinforced composite materials*. DEStech Publications, Inc, 2009.
- [16] I. A. Ibrahim, F. A. Mohamed, and E. J. Lavernia. Particulate reinforced metal matrix composites — a review. *Journal of Materials Science*, 26(5):1137–1156, 1991.
- [17] Bernard Jaffe. *Piezoelectric ceramics*, volume 3. Elsevier, 2012.
- [18] Robert M Jones. *Mechanics of composite materials*. CRC press, 1998.
- [19] Autar K Kaw. *Mechanics of composite materials*. CRC press, 2005.
- [20] JM Kiat and B Dkhil. Handbook of advanced dielectric, piezoelectric and ferroelectric materials, 2008.
- [21] Sidney B Lang. *Sourcebook of pyroelectricity*, volume 2. CRC Press, 1974.
- [22] George Lubin. *Handbook of composites*. Springer Science & Business Media, 2013.
- [23] Pankar K Mallick. *Fiber-reinforced composites: materials, manufacturing, and design*. CRC press, 2007.
- [24] A. Moropoulou, A. Bakolas, and S. Anagnostopoulou. Composite materials in ancient structures. *Cement and Concrete Composites*, 27(2):295 – 300, 2005. Cement and Concrete Research in Greece.
- [25] Hari Singh Nalwa. *Handbook of low and high dielectric constant materials and their applications, two-volume set*. Academic Press, 1999.

- [26] Jean-Pierre Pascault and Robert JJ Williams. *Epoxy polymers*. John Wiley & Sons, 2009.
- [27] Junuthula Narasimha Reddy. *Mechanics of laminated composite plates and shells: theory and analysis*. CRC press, 2004.
- [28] Roger M Rowell. *Handbook of wood chemistry and wood composites*. CRC press, 2012.
- [29] Md Rashedul H Sarker, Hasanul Karim, Ricardo Martinez, Diego Delfin, Rodrigo Enriquez, Mohammad Arif Ishtiaque Shuvo, Norman Love, and Yirong Lin. Temperature measurements using a lithium niobate (linbo 3) pyroelectric ceramic. *Measurement*, 75:104–110, 2015.
- [30] Gael Sebald, Daniel Guyomar, and Amen Agbossou. On thermoelectric and pyroelectric energy harvesting. *Smart Materials and Structures*, 18(12):125006, 2009.
- [31] Mailadil T Sebastian. *Dielectric materials for wireless communication*. Elsevier, 2010.
- [32] GM Sessler, J van Turnhout, B Gross, MG Broadhurst, GT Davis, S Mascarenhas, JE West, and R Gerhard-Multhaupt. Book metrics. *Topics in Applied Physics*, 33, 1987.
- [33] P Smith and J Yeomans. Benefits of fiber and particulate reinforcement. *Materials Science and Engineering*, 2:133–154, 2009.
- [34] Vinod Srinivasa, Vinay Shivakumar, Vinay Nayaka, Sunil Jagadeeshaiah, Murali Seetharam, Raghavendra Shenoy, and Abdelhakim Nafidi. Fracture morphology of carbon fiber reinforced plastic composite laminates. *Materials Research*, 13(3):417–424, 2010.
- [35] J.F. Tressler, S. Alkoy, A. Dogan, and R.E. Newnham. Functional composites for sensors, actuators and transducers. *Composites Part A: Applied Science and Manufacturing*, 30(4):477 – 482, 1999.
- [36] Ru-Min Wang, Shui-Rong Zheng, and Yujun George Zheng. *Polymer matrix composites and technology*. Elsevier, 2011.

- [37] Zuo-Guang Ye. *Handbook of advanced dielectric, piezoelectric and ferroelectric materials: Synthesis, properties and applications*. Elsevier, 2008.
- [38] Zhi Yu and Chen Ang. Maxwell-wagner polarization in ceramic composites  $\text{BaTiO}_3\text{-(Ni}_0.3\text{Zn}_0.7\text{Fe}_2\text{O}_4\text{)}$ . *Journal of applied physics*, 91(2):794–797, 2002.

## **Curriculum Vitae**

Emilio Tarango born February 25th of 1992, in Ciudad Delicias Chihuahua, at a young age he moved to Ciudad Jurez, Chihuahua. He commenced his upper division studies in El Paso, Texas at the El Paso Community College where he worked as a student manager for a successful student employee program. After two years of core courses, he transferred to The University of Texas at El Paso (UTEP) to pursue his degree in mechanical engineering. In the year of 2015, the month of May Emilio graduated Top Senior from his class with a Cum Lude honors recognition.

He received an invitation from the mechanical engineering chair at UTEP to joining the graduate school program, he accepted the invitation and began his master's of science in Mechanical Engineering where he obtained an employment position as a research assistant. The area where he devoted his master's degree was composites and embedded temperature sensors and energy harvests. Emilio also holds a pilot license with the ratings of multi-engine, instruments, and commercial privileges.

Permanent address: Fracc. Pueblo del Sol. Calle Pueblo de Tomochic 8406  
Ciudad Jurez, Chihuahua, 32545